THESIS FOR THE DEGREE OF DOCTOR OF PHILOSOPHY

Resources in quantum computation for discrete and continuous-variable systems

OLIVER HAHN

Department of Microtechnology and Nanoscience (MC2)
Applied Quantum Physics Laboratory
Chalmers University of Technology
Göteborg, Sweden, 2024

Resources in quantum computation for discrete and continuous-variable systems
OLIVER HAHN
ISBN 978-91-8103-059-4

Doktorsavhandlingar vid Chalmers tekniska högskola
Ny serie nr 5517
ISSN 0346-718X

Applied Quantum Physics Laboratory
Department of Microtechnology and Nanoscience (MC2)
Chalmers University of Technology
SE–412 96 Göteborg
Sweden
Telephone +46 (0)31-772 1000

Cover: The author's artistic rendition of computational resources in quantum computing.

Chalmers Digitaltryck
Göteborg, Sweden, 2024

Resources in quantum computation for discrete and continuous-variable systems

OLIVER HAHN
Applied Quantum Physics Laboratory
Department of Microtechnology and Nanoscience (MC2)
Chalmers University of Technology

Abstract

The evolution of information technology has reached a pivotal point with the emergence of quantum technology, promising unparalleled computational power and problem-solving capabilities. Quantum computing, based on discrete and continuous variables, promises the potential to solve computationally intractable problems efficiently. While discrete-variable quantum computing relies on qudits encoded in finite-dimensional Hilbert spaces, continuous-variable quantum computing exploits infinite-dimensional Hilbert spaces of harmonic oscillators. Both paradigms face challenges in achieving universality and fault tolerance, necessitating the exploration of resource theories such as non-Gaussianity and magic.

This thesis studies the resources for quantum computing for both discrete and continuous-variable systems and contributes to advancing our understanding of the resources essential for realizing the potential of quantum computing across different architectures. We investigate the interplay between these resource theories, proposing novel quantifiers and establishing connections between discrete and continuous-variable quantum computing.

Keywords: Quantum computing, quantum resource theory, continuous variables, discrete variables, resource theory of non-Gaussianity, resource theory of magic, Gottesman-Kitaev-Preskill code

Acknowledgments

This thesis has been made possible through the invaluable support and assistance of numerous individuals, to whom I extend my deepest gratitude.

First and foremost, I express my heartfelt appreciation to my supervisor, Giulia Ferrini. Your guidance and encouragement have shaped my journey throughout this PhD. I am grateful for your support of my academic pursuits and the freedom you granted me to explore my interests. I am equally indebted to my co-supervisors, Alessandro Ferraro and Laura García-Álvarez, whose patience and assistance have been a great help throughout my PhD. I want to deeply thank Patric Holmval for the great collaboration and hope we can continue our adventures in the future.

I extend my heartfelt thanks to Ryuji Takagi and Hayata Yamasaki for graciously hosting me during independent visits. Our collaborations have been enriching experiences, and I eagerly anticipate further collaborative endeavors in the future.

To the best office mate one can think of, Robert, I am profoundly grateful for our stimulating discussions and invaluable insights, especially regarding your very reasonable opinions and help with Matlab.

I am grateful to Alberto and Alex for their valuable feedback on this thesis, which significantly enhanced its quality and clarity.

I deeply appreciate my colleagues at AQP, whose camaraderie and support have made this journey immensely enjoyable. I extend my thanks to the entire AQP community, including the Sauna gang, the mountain mosses, the AQP cinematography club, and the ice cream breaks bunch, for their camaraderie and friendship.

To my family and friends, I owe a debt of gratitude for their unwavering support and encouragement throughout this endeavor.

Lastly, I want to thank my love, Therese, from the bottom of my heart, whose unwavering love and support have been my anchor throughout my postgraduate studies.

Oliver Hahn, Göteborg, May 2024

List of publications

This thesis is based on the following papers:

A Gaussian Conversion Protocols for Cubic Phase State Generation
Yu Zheng, Oliver Hahn, Pascal Stadler, Patric Holmval, Fernando Quijandría, Alessandro Ferraro, Giulia Ferrini
PRX Quantum **2**, 010327 (2021)

B Quantifying Qubit Magic Resource with Gottesman-Kitaev-Preskill Encoding
Oliver Hahn, Alessandro Ferraro, Lina Hultquist, Giulia Ferrini, Laura García-Álvarez
Phys. Rev. Lett. **128**, 210502 (2022)

C Deterministic Gaussian conversion protocols for non-Gaussian single-mode resources
Oliver Hahn, Patric Holmval, Pascal Stadler, Giulia Ferrini, Alessandro Ferraro
Phys. Rev. A **105**, 062446 (2022)

D Bridging non-Gaussian and magic resources via Gottesman-Kitaev-Preskill encoding
Oliver Hahn, Giulia Ferrini, Ryuji Takagi
In a draft at the time of printing

Other papers that are outside the scope of this thesis:

I Classical simulation and quantum resource theory of non-Gaussian optics
Oliver Hahn, Ryuji Takagi, Giulia Ferrini, Hayata Yamasaki
arXiv:2404.07115

Contents

Chapter 1

Introduction

1.1 Quantum Computing

The current world and our everyday lives have become unimaginable without information technology. Today, information technology stands at a turning point due to the rapid evolution of quantum technology, ushering in a new era that exploits fundamental quantum phenomena. Behind this development of information processing is the anticipation that quantum computers can tackle specific problems much more efficiently than their classical counterparts. Beyond simply speeding up computational problems, quantum computers could offer a way to solve problems that are intractable with classical means.

The most commonly studied paradigm for quantum computing or information processing assumes two-level systems – qubits – or, more generally, d-level systems – qudits. This approach encodes quantum information in finite-dimensional Hilbert spaces and is called *discrete variables* (DV). Many platforms are implementing this kind of quantum information processing, such as superconducting [1, 2], ion-trap-based [3], neutral atom[4] or NV center [5] architectures. Due to noise occurring in the physical implementations of the quantum processing, quantum error correction codes are necessary for a fault-tolerant quantum computer. The leading architectures for fault-tolerant quantum computers are based on stabilizer codes [6]. In this framework, only a non-universal subset of operations can be implemented transversally [7] —such that these operations do not propagate errors within a code block [8]. Transversal implementation is a simple way to implement a particular operation fault-tolerantly on the code subspace. The remaining operations required to obtain universality must be supplied non-transversally and are thus more challenging to perform. In $2d$ topological codes, the set of transversal or easy operations is called stabilizer operations, and it includes Clifford gates, preparation of stabilizer states, and computational basis measurements. Stabilizer operations alone cannot provide a quantum computational advantage, as the calcula-

tions composed only of stabilizer operations can be efficiently classically simulated [9]. Therefore, non-stabilizer operations must be implemented to recover universal quantum computing and leave the realm of classical computing. This is commonly done through magic state injection, which naturally leads to the so-called magic state model [10]. Preparing a high-fidelity magic state to obtain a high-fidelity magic gate is very costly in both qudits and gate operations as it involves magic state distillation [11, 12].

A different paradigm used for quantum computing uses the infinite-dimensional Hilbert spaces of harmonic oscillators and is called *continuous variables* (CV). In practical implementations, such as optics [13], microwave radiation [14–16], opto-mechanical systems [17–19], and atomic ensembles [20–23], some operations are more accessible to perform experimentally than others. The so-called Gaussian operations, like beamsplitters and rotations, are readily available in continuous-variable systems. While Gaussian operations are relatively straightforward to implement, they are insufficient for achieving universal quantum computing [24, 25]. Moreover, efficient classical simulation becomes possible when confined to Gaussian operations and states. Thus, incorporating non-Gaussian input, such as genuine quantum states like Fock states, becomes essential for achieving universal quantum computing and introducing computational challenges for classical simulation in continuous variables [26]. Furthermore, non-Gaussianity is required to perform error correction [27]. A significant feature of CV systems is their resilience to noise, showcased by the ability to implement cluster states composed of up to one-million modes [28] or to extend the lifetime of quantum information with respect to the constituents of the system [29]. In particular, their associated infinite dimensional Hilbert space can be exploited to host a variety of bosonic codes [30–33] — namely, sets of quantum states where logical digital information can be encoded redundantly to enable fault-tolerance against arbitrary errors. These codes showed impressive noise resilience in experimental implementations [2, 29, 34]. In particular, the use of superconducting cavities in the microwave regime has allowed for reaching the break-even point for error correction [29], meaning an enhancement in the lifetime of quantum information encoded in the state of the field using a rotationally symmetric bosonic code (RSB) [35] compared to an unencoded qubit using the same hardware.

Observing quantum phenomena in an experiment is challenging even today. The actual part of the experiment implementing a quantum computer, such as the superconducting circuit or the atoms, is tiny compared to the required shielding from the environment and the cooling apparatus [3, 36]. So, much care and effort are needed to see and conserve quantum behavior. This led to the idea of treating quantum phenomena as resources one uses to perform certain tasks. In this picture, the value of the resource is given by the difficulty of preparing it experimentally and the usefulness of the task, which is impossible to obtain classically. For example, entanglement is known to be helpful as a resource for a communication task called quantum teleportation.

As mentioned before, both paradigms to implement quantum computation, using discrete or continuous variables, have fundamental limitations in what operations can be performed. This fundamental separation between operations is dictated by experimental limitations. Within this framework, certain operations, such as Gaussian operations, are considered free, while the rest are deemed restricted or resourceful. The resource theoretic approach has provided deeper insights into entanglement and various other quantum phenomena [37–40]. It has also yielded practical applications, including improved simulation tools for qubit systems [41–45].

The two major resource theories we will investigate in this thesis that are relevant for quantum computing are the resource theory of non-Gaussianity and the resource theory of magic. As mentioned, non-Gaussianity is necessary to perform quantum computing in continuous-variable systems. Non-Gaussian features in e.g. quantum states can be quantified by several measures of non-Gaussianity [46–52], among which the negativity of Wigner function [48, 49, 53] has been known as the computable measure that also captures the hardness of classical simulability [54]. In the case of fault-tolerant quantum computers for discrete systems, the main difficulty is to obtain non-stabilizer operations [7]; thus, the leading resource is magic. Interestingly, the magicness of discrete-variable states can also be studied by looking at a discrete version of the Wigner function [55, 56] analogously to the case of continuous-variable systems. Indeed, the negativity of the discrete Wigner function [57, 58] is a valid magic measure when the underlying Hilbert space has odd dimensions. For even dimensions, one needs to consider other quantifiers [41–45, 59–62], as no known quasiprobability distribution easily connects to magic [63, 64].

The material presented in this thesis is primarily concerned with the resources important for quantum computing for both discrete and continuous-variable systems. Using Gaussian protocols, we study the inter-conversion of non-Gaussian resource states of interest for CV quantum computing. We contribute to the resource theory of magic by proposing a continuous variables-inspired quantifier and show a direct connection between the resource theory of magic and the resource theory of non-Gaussianity, the two main frameworks for discrete and continuous-variable quantum computing.

1.2 Overview of the thesis

The thesis is organized as follows. We start in Chap. 2 with an introduction to the basic concepts in quantum computing. We present the formalism for discrete-variable systems in Sec. 2.1 and for continuous-variable systems in Sec. 2.2. After that, we briefly introduce the framework of resource theories in Chap. 3. We discuss the general framework and then focus on the two central resource theoretic frameworks for quantum computing. In Sec. 3.2, we will review the resource theory of non-stabilizerness – or colloquially called $magic$ –, and in Sec. 3.3, the resource theory of genuine non-Gaussianity. In

Chap. 4, we discuss Gaussian conversion protocol between non-Gaussian states that are of interest for continuous-variable quantum computing. We start this chapter in Sec. 4.1 by presenting the framework we used to study the deterministic conversions of Paper A and Paper C. In Sec. 4.2, we give a small glimpse of the results of first Paper A and then Paper C. The contributions to the resource theory of magic and the definition of the quantifiers can be found in Chap. 5. We introduce our general approach and how we connected the resource theory of non-Gaussianity with the resource theory of magic in Sec. 5.1. In Sec. 5.2, we discuss the results of Paper B and the presented approach to study qubit systems. In Sec. 5.3, we provide the extension to arbitrary qudit dimensions and a classical simulation algorithm for qudits, providing a short glimpse of Paper D. At last, in Chap. 6, we summarize the thesis and the appended papers, including the main contributions, and finish with an outlook of future prospects.

Chapter 2

Basic concepts in quantum computing

Quantum computers promise to solve problems beyond the capabilities of classical computation [65–68]. In analogy to classical circuit logic, the circuit model is the most commonly used model for quantum computation. A universal quantum computer needs to be able to perform any unitary operator on an input states. Aside from unitary operations on some input, a quantum computation involves measurements. These measurements are often depicted at the end of the calculation since they will provide the computation's result. However, especially in the case of error correction codes, measurements are done during the application of the quantum circuit to extract error syndromes and then apply an appropriate unitary to correct the error. We show a quantum circuit in Fig. 2.1.

In this thesis, we will focus on two different quantum computing paradigms. In the first one, referred to as *discrete-variable* quantum computing, the informational building blocks are $d-$level systems. This is the most commonly studied paradigm, with $d = 2$ yielding the case of qubit-based quantum computing. The other uses the infinite Hilbert space of a harmonic oscillator to encode quantum information. Since relevant observables in this paradigm have a continuous spectrum, this approach is called *continuous-variable* quantum computing. This chapter is organized as follows. First, we will introduce the basic concept required for quantum information processing using d-level systems. Then, we will discuss the *continuous variables* paradigm and focus on Gaussian operations.

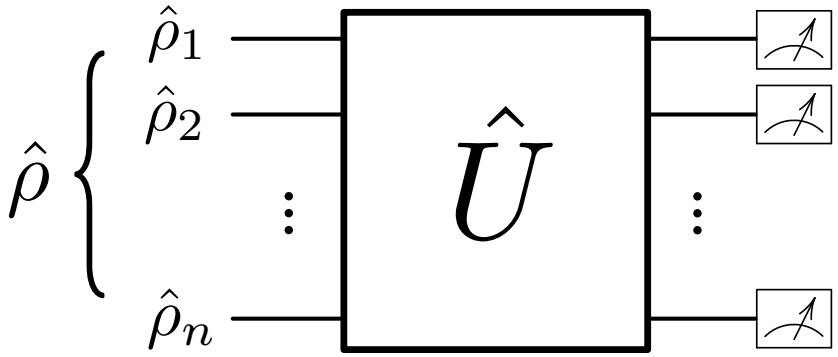

Figure 2.1: A quantum circuit involving n basis building blocks that can be qudits or quantum modes represented by horizontal lines. After the states $\hat{\rho}_1, ..., \hat{\rho}_n$ are initialized, unitary operations are applied to the quantum states. Mid-circuit measurements and feed-forward operations can be applied as well. In the end, local measurements are performed.

2.1 Discrete-variable Quantum Computing

Qubits, i.e., 2-level systems, are usually assumed if one speaks colloquially about quantum computing. This is not necessary. Different Hilbert space structures can be used for quantum computation or, more generally, quantum information processing. Qudits are, for example, intuitive generalizations of qubits to d dimensions. In the following, we review quantum computing using qudits.

2.1.1 Clifford quantum computation

A general pure qudit state is defined as

$$|\psi\rangle = \sum_{i=0}^{d-1} \alpha_i |i\rangle \tag{2.1}$$

with normalization condition $\sum_{i=0}^{d-1} |\alpha_i|^2 = 1$ and $|i\rangle$ a computational basis state. The Pauli operators for qubits are well-known

$$Z_2 = \begin{pmatrix} 1 & 0 \\ 0 & -1 \end{pmatrix} \tag{2.2}$$

$$X_2 = \begin{pmatrix} 0 & 1 \\ 1 & 0 \end{pmatrix}. \tag{2.3}$$

We wrote here the matrix representation of $\hat{X}_2, \hat{Z}_2$ and thus omitted the hats. These two operators generate a group, the so-called Pauli group. The Pauli group can be defined for arbitrary dimensions in analogy to the qubit case as
$\mathcal{P}_d = \left\{\omega_D^u \hat{X}_d^v \hat{Z}_d^w : v, w \in \mathbb{Z}_d, u \in \mathbb{Z}_D\right\}$ where $\omega_D = \mathrm{e}^{2\pi \mathrm{i}/D}$ is the D th root of unity and

$$D = \begin{cases} d: & \text{for } d \text{ odd} \\ 2d: & \text{for } d \text{ even} \end{cases} \tag{2.4}$$

with $\mathbb{Z}_d$ being the integers modulo d. The d dimensional Pauli operators $\hat{Z}_d, \hat{X}_d$, sometimes also called shift and clock operators, are a way to generalize the qubit Pauli operators $\hat{Z}_2, \hat{X}_2$ and are defined as

$$\hat{X}_d = \sum_{j=0}^{d-1} |j+1\rangle \langle j| \tag{2.5}$$

$$\hat{Z}_d = \sum_{j=0}^{d-1} \omega_d^j |j\rangle \langle j| \tag{2.6}$$

with the property $\hat{X}_d^d = \hat{Z}_d^d = \mathbb{1}$ [69].

We use the generalized Pauli operators $\hat{X}_d, \hat{Z}_d$ to define the operators of the d-dimensional Heisenberg-Weyl group as [55, 56]

$$\hat{P}_d(a,b) = \omega_D^{\frac{1}{2}ab} \hat{X}_d^a \hat{Z}_d^b \tag{2.7}$$

with $a, b \in \mathbb{Z}_d$. The commutation relations between two discrete Heisenberg-Weyl operators are

$$\hat{P}_d(a,b)\hat{P}_d(c,d) = \omega_d^{(a,b)\Omega(c,d)^T} \hat{P}_d(c,d)\hat{P}_d(a,b), \tag{2.8}$$

where

$$\Omega = \begin{pmatrix} 0 & 1 \\ -1 & 0 \end{pmatrix} \tag{2.9}$$

is the symplectic form for one qudit.

Heisenberg-Weyl operators of multi, let's say n, qudit systems are just tensor products of single Heisenberg-Weyl operators. We will write them as

$$\hat{P}_d(\boldsymbol{u}) = \bigotimes_{i=1}^{n} \hat{P}_d(a_i, b_i) \tag{2.10}$$

with $\boldsymbol{u} = (\boldsymbol{a}, \boldsymbol{b}) \in \mathbb{Z}_d^{2n}$. As it is widely known for the case of qubits, they fulfill the orthogonality relations

$$\mathrm{Tr}\left[\hat{P}_d(\boldsymbol{u})\hat{P}_d^\dagger(\boldsymbol{v})\right] = d^n \delta_{\boldsymbol{u},\boldsymbol{v}}. \tag{2.11}$$

Clifford unitary operators U_C are defined as the unitary operators that map the Pauli group into the Pauli group. In consequence, a Clifford unitary acts on the Heisenberg-Weyl operator in a simple way

$$\hat{U}_C \hat{P}_d(\boldsymbol{u})\hat{U}_C^\dagger = \hat{P}_d(S\boldsymbol{u}) \tag{2.12}$$

where $S \in \mathrm{Sp}(2n, \mathbb{Z}_D)$ is a symplectic matrix. The following unitary operations or gates generate the $n-$qudit Clifford group

$$\hat{R} = \sum_{j,s=0}^{d-1} \omega_d^{js} \left|s\right\rangle\!\left\langle j\right| \tag{2.13}$$

$$\hat{P} = \sum_{j=0}^{d-1} \omega_d^{j^2/2} (\omega_D \omega_{2d}^{-1})^{-j} \left|j\right\rangle \left\langle j\right| \tag{2.14}$$

$$\hat{\mathrm{SUM}} = \sum_{i,j=0}^{d-1} \left|i\right\rangle\!\left\langle i\right| \otimes \left|i + j \mod d\right\rangle\!\left\langle j\right|. \tag{2.15}$$

For $d = 2$, these operators reduce to the Hadamard, Phase or sometimes called S, and CNOT gate [69] respectively.

2.1.2 Characteristic and Wigner functions for discrete-variable systems

As noted before, Heisenberg-Weyl operators fulfill orthogonality relations and thus form a basis for operators. Using the discrete Heisenberg-Weyl operators as a basis, we define the characteristic function [56] as

$$\chi_{\hat{\rho}}^{\mathrm{DV}}(\boldsymbol{u}) = d^{-n}\,\mathrm{Tr}\left[\hat{\rho}\hat{P}_d(\boldsymbol{u})^\dagger\right]. \tag{2.16}$$

In Fig. 2.2, we show the characteristic function for a qubit. This is equivalent to the Bloch-sphere representation since the expectation values of Pauli operators are on the axis. This representation allows one to see immediately if a state is a stabilizer state or not by comparing whether it is inside the stabilizer polytope.

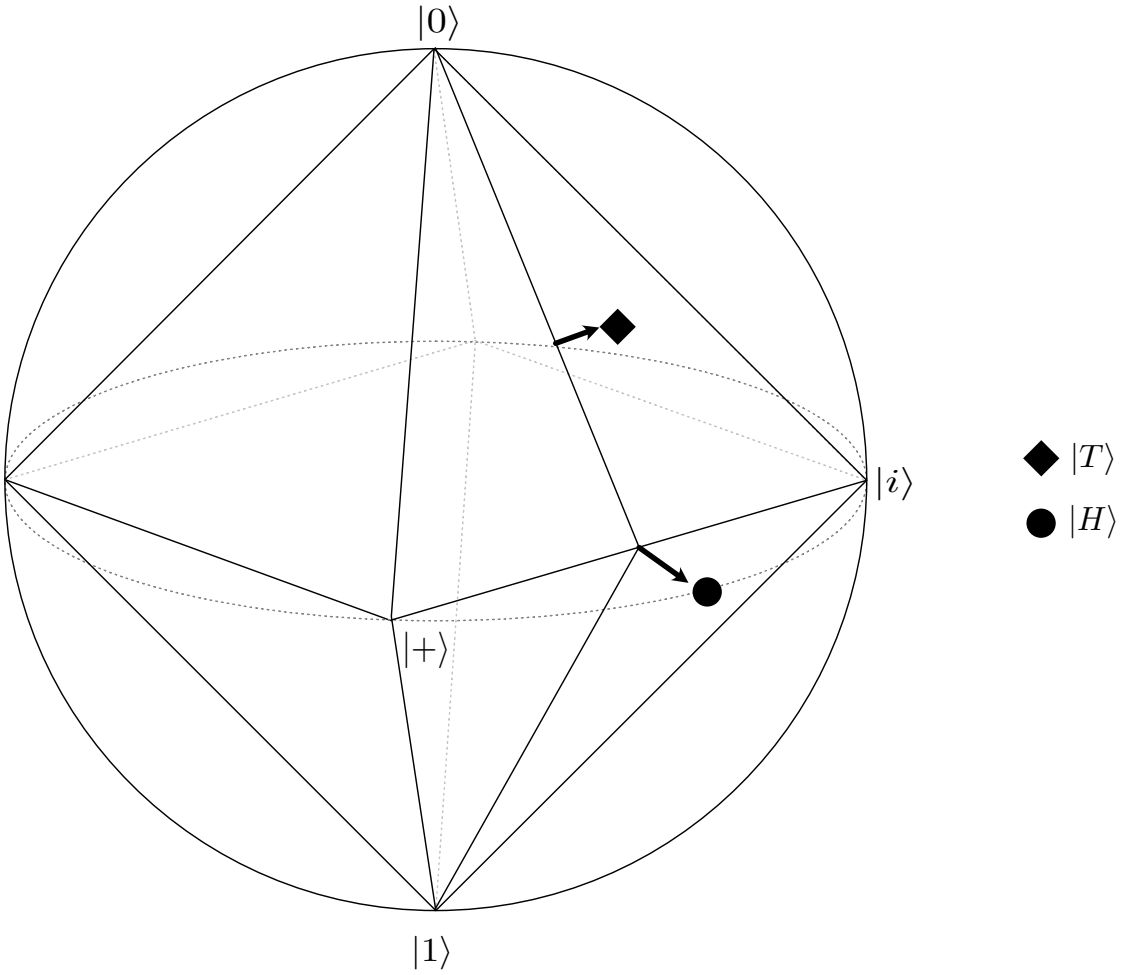

Figure 2.2: The discrete characteristic function for qubits can be represented in the Bloch sphere. The sketched octahedron is called the stabilizer octahedron. All stabilizer states are the intersection of the octahedron and the sphere. Marked are the H-type and $T-$type magic states. The $H-$type magic states are on the sphere orthogonal to an edge, and the $T-$type magic states are on the sphere orthogonal to a facet of the stabilizer octahedron.

Odd-dimensional systems allow for a simple way to define the discrete Wigner function by the discrete symplectic Fourier transform of the characteristic function:

$$W_{\hat{\rho}}^{\mathrm{DV}}(\boldsymbol{u}) = d^{-n} \sum_{\boldsymbol{v}\in\mathbb{Z}_d^{2n}} \omega_d^{-\boldsymbol{u}\Omega_n\boldsymbol{v}^T} \chi_{\hat{\rho}}^{\mathrm{DV}}(\boldsymbol{v}) \tag{2.17}$$

$$= d^{-n} \operatorname{Tr}\left[\hat{A}(\boldsymbol{u})\hat{\rho}\right], \tag{2.18}$$

where Ω_n now takes the form

$$\Omega_n = \begin{pmatrix} 0 & \mathbb{1}_n \\ -\mathbb{1}_n & 0 \end{pmatrix} \tag{2.19}$$

and $\mathbb{1}_n$ is the $n \times n$ identity matrix. The phase space point operator in Eq. (2.15) can be written as

$$\hat{A}(\boldsymbol{u}) = d^{-n} \sum_{\boldsymbol{v}\in\mathbb{Z}_d^{2n}} \omega_d^{-\boldsymbol{u}\Omega_n\boldsymbol{v}^T} \hat{P}_d(\boldsymbol{u})^\dagger. \tag{2.20}$$

The discrete Wigner function in odd dimensions has many useful properties. It is covariant under Clifford unitaries U_C, meaning that

$$W_{\hat{U}_C\rho\hat{U}_C^\dagger}^{\mathrm{DV}}(\boldsymbol{u}) = W_{\hat{\rho}}^{\mathrm{DV}}(S\boldsymbol{u}) \tag{2.21}$$

with $S \in \mathrm{Sp}(2n, \mathbb{Z}_d)$ being the symplectic matrix associated with Clifford unitary U_C.

The discrete Wigner function $W_{\hat{\rho}}(\boldsymbol{u})$ is a quasiprobability distribution and is thus not necessarily positive. Nevertheless, it yields a valid probability distribution for an arbitrary stabilizer state.

2.1.3 Universality in discrete-variable quantum computing and magic states

The set of Clifford unitary operators is not universal; we cannot decompose any unitary into Clifford operations only. We can complete the gates set required to decompose any unitary by adding one more gate. A common choice for qubits is the T-gate,

$$T = \begin{pmatrix} 1 & 0 \\ 0 & \mathrm{e}^{\mathrm{i}\frac{\pi}{4}} \end{pmatrix}, \tag{2.22}$$

here represented in the computational basis. However, one can choose different unitary operators to get a universal gate set together with Clifford gates. For qudits, commonly

the d dimensional analog of the Toffoli gate

$$\hat{\text{Tof}} = \sum_{i,j,k=0}^{d-1} |i\rangle\langle i| \otimes |j\rangle\langle j| \otimes |k + ij\rangle \langle k| \,. \tag{2.23}$$

is chosen as the non-Clifford gate.

Many error correction codes can be understood using *stabilizers* [70]. If a state $|\psi\rangle$ is the $+1$ eigenstate of an operator $\hat{U}$, we say that the state $|\psi\rangle$ is stabilized by $\hat{U}$. *Stabilizer codes* are quantum error correction codes where the valid code words are stabilized by $n - k$ distinct commuting Pauli operators, where n is the number of physical qubits, and k is the number of encoded qudits. These Pauli operators generate a d^{n-k} dimensional Abelian group, the so-called *stabilizer group*. The stabilizer group, in turn, stabilizes a d^k dimensional subspace of the whole $n-$qudit Hilbert space, called the coding space [9]. This subspace contains all valid codewords of the codes. By measuring the $n-k$ generators of the stabilizer group, we can obtain an error syndrome and then identify which error occurred for appropriately chosen codes.

Definition 1. *A pure stabilizer state is a state that is fully determined by a stabilizer group S,i.e.*

$$g_i |\psi\rangle = |\psi\rangle \tag{2.24}$$

for $g_i \in S$ where card$(S) = d^n$. A d^n dimensional stabilizer group stabilizes a subspace of one qudit.

The most prominent non-stabilizer –or colloquially called magic – states for qubits are the T and the H state

$$|H\rangle = \frac{1}{\sqrt{2}}\Big(|0\rangle + \mathrm{e}^{\mathrm{i}\pi/4} |1\rangle\Big) \tag{2.25}$$

$$|T\rangle = \cos(\beta) |0\rangle + \sin(\beta)\mathrm{e}^{\mathrm{i}\pi/4} |1\rangle \tag{2.26}$$

with $\cos(2\beta) = \frac{1}{\sqrt{3}}$.

2.2 Continuous-variable Quantum Computing

A related but inherently different paradigm in quantum information processing uses infinite dimensional systems. The central observables in these systems are the position $\hat{q}$ and momentum $\hat{p}$ operators that fulfill the canonical commutation relations

$$[\hat{q}, \hat{p}] = \mathrm{i}. \tag{2.27}$$

These operators have continuous spectra, which is why this type of quantum information processing is often called *continuous-variable* quantum computing and in contrast to *discrete-variable* quantum computing systems described in the previous section. We are going to indicate the vector of quadrature operators for n bosonic modes as $\hat{\boldsymbol{r}} = (\hat{q}_1, \hat{p}_1 ... \hat{q}_n, \hat{p}_n)^T$, and for each mode we use the following convention for the relation between the quadrature operators and the creation and annihilation operators: $\hat{q} = (\hat{a} + \hat{a}^\dagger)/\sqrt{2}$ and $\hat{p} = (\hat{a} - \hat{a}^\dagger)/(\sqrt{2}i)$, corresponding to setting $\hbar = 1$.

2.2.1 Gaussian quantum optics

Gaussian quantum optics has a wide range of applications. Beyond its vast use, which spans from quantum metrology to quantum key distribution, an appealing feature of Gaussian quantum optics is that several analytical techniques are available in this regime. Here, we introduce this thesis's main notations and formalism regarding Gaussian quantum optics.

Definition 2 (Gaussian unitaries)**.** *Gaussian unitaries are defined as*

$$\hat{U} = \boldsymbol{e}^{i\hat{H}_G} \tag{2.28}$$

$$\hat{H}_G = \frac{1}{2}\hat{\boldsymbol{r}}^T \boldsymbol{H} \hat{\boldsymbol{r}} + \bar{\boldsymbol{r}}\hat{\boldsymbol{r}} \tag{2.29}$$

where we use the shorthand notation $\hat{\boldsymbol{r}} = (\hat{q}_1, \hat{p}_1, ..., \hat{q}_n, \hat{p}_n)^T$ for the vector of canonical operators and $\bar{\boldsymbol{r}} = (r_{q_1}, r_{p_1}, ... r_{q_n}, r_{p_n})^T$ a vector of real numbers and H is a $2n \times 2n$ symmetric matrix.

The commonly used squeezing, displacement, and phase rotation operators, as well as the beamsplitter, are all special cases of Gaussian unitaries.

For a n-mode system, the infinite-dimensional Heisenberg-Weyl operators, which are often called displacement operators for infinite-dimensional systems, are defined as

$$\hat{D}(\boldsymbol{r}) = \prod_{j=1}^{n} \mathrm{e}^{-\mathrm{i}r_{p_j} r_{q_j}/2} \mathrm{e}^{-\mathrm{i}r_{q_j}\hat{p}_j} \mathrm{e}^{\mathrm{i}r_{p_j}\hat{q}_j} \tag{2.30}$$

where $\boldsymbol{r} = (r_{q_1}, ..., r_{q_n}, r_{p_1}, ..., r_{p_n}) = (\boldsymbol{r_q}, \boldsymbol{r_p})$ and $\hat{q}_j$, $\hat{p}_j$ are position and momentum operators for j th mode. Displacement operators fulfill the commutation relation

$$\hat{D}(\boldsymbol{r})\hat{D}(\boldsymbol{r'}) = \mathrm{e}^{-\mathrm{i}\boldsymbol{r}\Omega_n \boldsymbol{r'}^T} \hat{D}(\boldsymbol{r'})\hat{D}(\boldsymbol{r}). \tag{2.31}$$

Note that they fulfill equivalent commutation relations compared to the discrete Heisenberg-Weyl operator. The difference lies in the phase factor e^{i} instead of ω_d.

Beyond displacements, other notable Gaussian unitary operators are the squeezing $\hat{S}(\xi)$ and the phase rotation $\hat{U}_p(\gamma)$ operators, which are defined respectively as

$$\hat{S}(\xi) = \mathrm{e}^{-\mathrm{i}\frac{\xi}{2}(\hat{q}\hat{p}+\hat{p}\hat{q})}, \tag{2.32}$$

$$\hat{U}_p(\gamma) = \mathrm{e}^{-\mathrm{i}\gamma\hat{n}} = \mathrm{e}^{-\mathrm{i}\frac{\gamma}{2}(\hat{q}^2+\hat{p}^2)}, \tag{2.33}$$

with $\hat{n}$ being the photon number operator, $\gamma \in \mathbb{R},\ \xi \in \mathbb{C}$. Phase rotation, squeezing, and displacement operators are enough to decompose any single-mode Gaussian unitary.

To decompose multimode Gaussian unitaries, an additional 2-mode unitary is sufficient:

$$\hat{U}_{BS}(\theta) = \mathrm{e}^{\theta(\hat{a}_1^\dagger\hat{a}_2-\hat{a}_1\hat{a}_2^\dagger)} = \mathrm{e}^{\mathrm{i}\theta(\hat{q}_1\hat{p}_2+\hat{p}_1\hat{q}_2)}, \tag{2.34}$$

Which amounts to the unitary action of a beamsplitter. The angle θ sets the transmissivity of the beamsplitter $\tau = \cos(\theta)^2$, which is called balanced if $\tau = \frac{1}{2}$ or equivalently $\theta = \frac{\pi}{4}$.
Similar to Gaussian unitaries, we can define Gaussian states.

Definition 3 (Gaussian states)**.** *A Gaussian state is defined as*

$$\hat{\rho}_G = \frac{e^{-\beta\hat{H}_G}}{\mathrm{Tr}\left[e^{-\beta\hat{H}_G}\right]} \tag{2.35}$$

including the case $\beta \to \infty$ which yields pure states. For pure states, this is equivalent to

$$|\psi_G\rangle = \hat{U}_G\,|0\rangle \tag{2.36}$$

$$= \hat{U}_L\hat{S}(\boldsymbol{\xi})\hat{D}(\boldsymbol{\alpha})\,|0\rangle\,, \tag{2.37}$$

we used the fact that passive Gaussian unitary operators map the vacuum state to itself.

The advantage of Gaussian states is that they are fully determined by the mean

$$\bar{\boldsymbol{r}} = \mathrm{Tr}[\hat{\boldsymbol{r}}\hat{\rho}_G] \tag{2.38}$$

and the covariance matrix

$$\sigma = \mathrm{Tr}\left[\{(\hat{\boldsymbol{r}}-\bar{\boldsymbol{r}}),(\hat{\boldsymbol{r}}-\bar{\boldsymbol{r}})^T\}\hat{\rho}_G\right] \tag{2.39}$$

where $\{,\}$ is the anti-commutator, and $\boldsymbol{r}\boldsymbol{r}^T$ is the outer product. The requirement on all covariance matrices is

$$\sigma \pm \mathrm{i}\Omega \geq 0. \tag{2.40}$$

Using the covariance matrix formalism, one can efficiently compute the dynamics of a quantum state as long as the operations involved are Gaussian. Gaussian operations refer to any operations composed of preparation of Gaussian states, applications of Gaussian unitaries, and measurement by homodyne or heterodyne detection. Below, we summarize how the covariance matrix evolves [71] under Gaussian transformations. By observing how the mean transforms, we can deduce how the canonical operators $\hat{\boldsymbol{r}}$ transform.

Action of Gaussian unitaries Displacement operations by $\bar{\boldsymbol{r}}'$ have the following action on the mean and the covariance matrix:

$$\bar{\boldsymbol{r}} \to \bar{\boldsymbol{r}} + \bar{\boldsymbol{r}}', \tag{2.41}$$

$$\sigma \to \sigma. \tag{2.42}$$

A general symplectic transformation $\hat{S}$ is acting as

$$\bar{\boldsymbol{r}} \to S\bar{\boldsymbol{r}}, \tag{2.43}$$

$$\sigma \to S\sigma S^T. \tag{2.44}$$

One can immediately get the symplectic matrix and the displacement from the Gaussian unitary. $\bar{\boldsymbol{r}}$ is directly the displacement while the symplectic matrix is given by $\mathrm{e}^{\Omega H}$.

There are parameterizations for symplectic transformations [72]. Any (multimode) Gaussian unitary can, as a consequence of the Euler decomposition, be decomposed as

$$\hat{U}_G = \hat{U}_L \hat{S}(\boldsymbol{\xi}) \hat{D}(\boldsymbol{\alpha}) \hat{V}_L, \tag{2.45}$$

where $\hat{U}_L$ and $\hat{V}_L$ are passive Gaussian unitary operators, the the L stands fir "linear optics". One can summarize all unitaries that a quadratic Hamiltonian generates as the symplectic unitaries or transformations. $\hat{U}_L, \hat{V}_L, \hat{S}(\boldsymbol{\xi})$ are examples of symplectic transformations.

Action of Tensor products and partial trace Suppose that we have a two-mode Gaussian state with

$$\bar{\boldsymbol{r}} = \bar{\boldsymbol{r}}_{\boldsymbol{A}} \oplus \bar{\boldsymbol{r}}_{\boldsymbol{B}} = \begin{pmatrix} \bar{\boldsymbol{r}}_{\boldsymbol{A}} \\ \bar{\boldsymbol{r}}_{\boldsymbol{B}} \end{pmatrix}, \tag{2.46}$$

$$\sigma = \sigma_A \oplus \sigma_B = \begin{pmatrix} \sigma_A & 0 \\ 0 & \sigma_B \end{pmatrix}. \tag{2.47}$$

Then, the partial trace on the second subsystem yields

$$\bar{\boldsymbol{r}} \to \bar{\boldsymbol{r}}_{\boldsymbol{A}}, \tag{2.48}$$

$$\sigma \to \sigma_A. \tag{2.49}$$

Gaussian completely positive and trace-preserving (CPTP) map Given a Gaussian initial state with covariance σ and mean $\bar{\boldsymbol{r}}$, the evolution of a Gaussian CPTP map is characterized by two real matrices X, Y and a vector $\boldsymbol{d}$ as

$$\bar{\boldsymbol{r}} \to X\bar{\boldsymbol{r}} + \boldsymbol{d}, \tag{2.50}$$

$$\sigma \to X\sigma X^T + Y, \tag{2.51}$$

with the requirement that

$$Y + \mathrm{i}\Omega \geq \mathrm{i}X\Omega X^T. \tag{2.52}$$

2.2.2 Characteristic and Wigner function for continuous-variable systems

It is widespread to use phase-space representations to represent continuous-variable states. They are equivalent to the density operator formalism but are often easier to handle and allow for visualization. The phase-space representation we will use is the continuous Wigner function.

Similarly to the discrete case, we can use the continuous Heisenberg-Weyl operators to define the characteristic function

$$\chi_{\hat{\rho}}^{\mathrm{CV}}(\boldsymbol{r}) = \mathrm{Tr}\left[\hat{\rho}\hat{D}(-\boldsymbol{r})\right] \tag{2.53}$$

and the Wigner function as its symplectic Fourier transform

$$W_{\hat{\rho}}^{\mathrm{CV}}(\boldsymbol{r}) = \frac{1}{(2\pi^2)^n}\int_{\mathbb{R}^{2n}} \mathrm{d}\boldsymbol{r'}\mathrm{e}^{\mathrm{i}\boldsymbol{r}\Omega_n\boldsymbol{r'}}\chi_{\hat{\rho}}(\boldsymbol{r'}) \tag{2.54}$$

$$= \left(\frac{1}{2\pi}\right)^n \int_{\mathbb{R}^n} \mathrm{d}\boldsymbol{x}\mathrm{e}^{\mathrm{i}\boldsymbol{r_p}\boldsymbol{x}} \left\langle \boldsymbol{r_q} + \frac{\boldsymbol{x}}{2}\middle|\, \hat{\rho} \,\middle| \boldsymbol{r_q} - \frac{\boldsymbol{x}}{2}\right\rangle_{\hat{q}}. \tag{2.55}$$

The Wigner function is a quasiprobability distribution. This means that the Wigner function can be negative in parts. These negative regions are small, only a few $\hbar$ in size. Smoothing a Wigner function by a filter of size larger than $\hbar$ (e.g., convolving with a phase-space Gaussian) results in a positive Wigner function, i.e., it may be thought to have been averaged to a classical probability distribution [73]. An example is the transition from the Wigner function to the Husimi-Q function, which is positive everywhere.

In this thesis, we use many properties of the characteristic and the Wigner function. The property that $\hat{\rho}$ is a hermitian operator leads to the fact that the Wigner function $W_{\hat{\rho}}^{\mathrm{CV}}(\boldsymbol{r}) \in \mathbb{R}$ and $\mathrm{Tr}[\hat{\rho}] = 1$ leads to the normalization of the Wigner function

$$\int_{\mathbb{R}^{2n}} \mathrm{d}\boldsymbol{r} W_{\hat{\rho}}^{\mathrm{CV}}(\boldsymbol{r}) = 1. \tag{2.56}$$

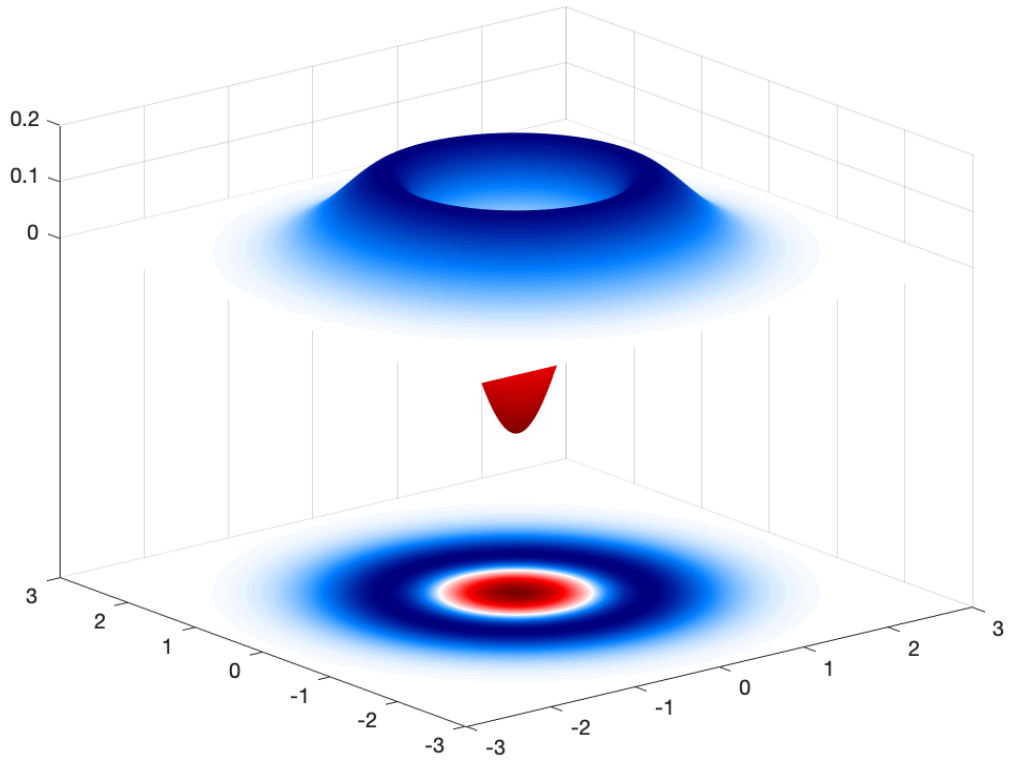

Figure 2.3: Wigner function of a Fock state $|1\rangle$. In the top part, we can see the Wigner function as a 3-dimensional object with the colors accentuating the values, with blue being a positive number and red being a negative number. On the bottom, one can see the projection in two dimensions, with the values of the Wigner function encoded in color.

A standard measure of closeness or similarity of quantum states is the fidelity [74]

$$\mathcal{F}(\hat{\rho}_1, \hat{\rho}_2) = \left(\mathrm{Tr}\left\{ \sqrt{\sqrt{\hat{\rho}_1}\hat{\rho}_2\sqrt{\hat{\rho}_1}} \right\} \right)^2. \tag{2.57}$$

The fidelity of an arbitrary state $\hat{\rho}$ and a pure state $|\Psi\rangle\langle\Psi|$ can be written using the Wigner functions as

$$\mathcal{F}(\hat{\rho}, |\Psi\rangle\langle\Psi|) = \int_{\mathbb{R}^{2n}} \mathrm{d}\boldsymbol{r} W^{\mathrm{CV}}_{\hat{\rho}}(\boldsymbol{r}) W^{\mathrm{CV}}_{|\Psi\rangle\langle\Psi|}(\boldsymbol{r}). \tag{2.58}$$

The action of Gaussian unitaries $\hat{U}_G$ changes the Wigner function in the following way:

$$W^{\mathrm{CV}}_{\hat{U}_G\hat{\rho}\hat{U}_G^\dagger}(\boldsymbol{r}) = W^{\mathrm{CV}}_{\hat{\rho}}(S^{-1}\boldsymbol{r} - S^{-1}\boldsymbol{d}) \tag{2.59}$$

where $\boldsymbol{d}$ describes the displacement and S the symplectic matrix. Gaussian states have a positive Wigner function and can be written as

$$W_{\hat{\rho}_G}(\boldsymbol{r}) = \frac{2^n}{\pi^n\sqrt{\det[\sigma]}} \mathrm{e}^{-(\boldsymbol{r}-\bar{\boldsymbol{r}})\sigma^{-1}(\boldsymbol{r}-\bar{\boldsymbol{r}})}. \tag{2.60}$$

The characteristic function fulfills the following property since $\hat{\rho}$ is a hermitian operator

$$\chi^{\mathrm{CV}}_{\hat{\rho}}(\boldsymbol{r}) = \chi^{\mathrm{CV}*}_{\hat{\rho}}(-\boldsymbol{r}). \tag{2.61}$$

The property of $\mathrm{Tr}[\hat{\rho}] = 1$ leads to

$$\chi^{\mathrm{CV}}_{\hat{\rho}}(0) = 1. \tag{2.62}$$

The positivity of ρ is a bit more complicated to show; we have that $\rho \geq 0$ if and only if the matrix

$$D_{ij} = \chi^{\mathrm{CV}}_{\hat{\rho}}(\boldsymbol{r}_j - \boldsymbol{r}_j)\mathrm{e}^{\mathrm{i}\boldsymbol{r}_j^T\Omega\boldsymbol{r}_i} \tag{2.63}$$

is positive semi-definite for all sets of vectors $R = \{\boldsymbol{r}_i : \boldsymbol{r}_i \in \mathbb{R}^{2n}\}$.

The characteristic function of a Gaussian state ρ_G with covariance matrix σ and mean $\bar{\boldsymbol{r}}$ is

$$\chi^{\mathrm{CV}}_{\hat{\rho}_G}(\boldsymbol{r}) = \mathrm{e}^{\frac{1}{4}\boldsymbol{r}^T\Omega^T\sigma\Omega\boldsymbol{r}}\mathrm{e}^{\mathrm{i}\boldsymbol{r}\Omega\bar{\boldsymbol{r}}}. \tag{2.64}$$

The characteristic function allows for a concise mathematical description of the action of Gaussian operations. The characteristic function transforms under displacements as:

$$\chi_{\hat{\rho}}(\boldsymbol{r})^{\mathrm{CV}} \rightarrow \chi^{\mathrm{CV}}_{\hat{D}(\boldsymbol{d})\hat{\rho}\hat{D}(\boldsymbol{d})^{\dagger}}(\boldsymbol{r}) = \mathrm{e}^{\mathrm{i}\boldsymbol{d}^T\Omega\boldsymbol{r}}\chi^{\mathrm{CV}}_{\hat{\rho}}(\boldsymbol{r}). \tag{2.65}$$

This directly follows from the definition of the characteristic function and the commutation relations of Heisenberg-Weyl operators.

The characteristic function allows one to write explicitly the action of Gaussian CPTP maps and parameterize the action of such maps. Beyond unitary deterministic processes, these Gaussian maps may also include non-unitary maps representing noise or processes where auxiliary modes are measured. In the latter case, however, feed-forward is assumed to restore determinism.

The action of a general Gaussian CPTP-map Φ on the characteristic function can then be written as [75]

$$\chi_{\hat{\rho}}(\boldsymbol{r}) \rightarrow \chi_{\Phi(\hat{\rho})}(\boldsymbol{r}) = \mathrm{e}^{-\frac{1}{4}\boldsymbol{r}^T\Omega^T Y\Omega\boldsymbol{r}+\mathrm{i}\boldsymbol{d}^T\Omega\boldsymbol{r}}\chi_{\hat{\rho}}(\Omega^T X^T\Omega\boldsymbol{r}), \tag{2.66}$$

with X,Y being 2×2 real matrices, $\boldsymbol{d}$ being a 2-dimensional real vector, Y being symmetric and fulfilling the following positive semi-definite matrix constraint

$$Y \pm \mathrm{i}(\Omega - X\Omega X^T) \geq 0\ . \tag{2.67}$$

Notice that Eq. (2.67) implies that Y has to be a positive semi-definite matrix. The requirement for positive semi-definiteness needs to hold for both signs since transposition does not influence a matrix's positive (semi-) definiteness. Symplectic transformations are special cases of the protocols introduced in Eq. (2.66) and correspond to the case where the matrix Y is set to zero, whereas $X \in \mathrm{Sp}(2,\mathbb{R})$ is then a symplectic matrix [71].

We can rewrite the fidelity for the characteristic function for an arbitrary state ρ and a pure state $|\Psi\rangle\langle\Psi|$ as

$$\begin{aligned}\mathcal{F}(\hat{\rho}, |\Psi\rangle\langle\Psi|) &= \langle\Psi|\,\hat{\rho}\,|\Psi\rangle \\ &= \frac{1}{4\pi}\int_{\mathbb{R}^{2n}} \mathrm{d}\boldsymbol{r}\ \chi_{\hat{\rho}}(\boldsymbol{r})\ \chi_{|\Psi\rangle\langle\Psi|}(-\boldsymbol{r}).\end{aligned} \tag{2.68}$$

While the integration is over an infinite Hilbert space, the characteristic function tends rapidly to zero within a relatively small region.

2.2.3 Universality in continuous-variable quantum computing and non-Gaussian states

Despite the richness of Gaussian quantum optics, it is not universal, meaning we cannot represent all possible states and operations using the Gaussian manifold. Even worse,

if one only considers Gaussian operations and Gaussian states, one cannot have an exponential quantum computational advantage since this scenario can be efficiently simulated classically using the covariance matrix formalism [76]. Thus, we must add non-Gaussian operations or states to obtain genuine quantum phenomena beyond classical simulatability. The setting of Gaussian quantum information processing is moreover limited by several no-goes for many tasks, including entanglement distillation [77–79], error correction [27], quantum computation [80] and violation of Bell inequalities/contextuality [81].

We can talk about two different notions of universality in continuous variables. The first can be seen as the infinite-dimensional version of what we discussed in the previous section. Namely, we can approximate any unitary operation of our choosing stemming from evolution under arbitrary Hamiltonians that are polynomials of $\hat{q}, \hat{p}$. We require a so-called non-Gaussian unitary. The standard choice is the so-called cubic-phase gate

$$\hat{C}(c) = \mathrm{e}^{\mathrm{i}c\hat{q}^3}. \tag{2.69}$$

We can use the cubic phase gate and Gaussian unitary operations to represent any unitary generated by polynomials of $\hat{q}, \hat{p}$ [80]. If we apply two unitary operators $\mathrm{e}^X, \mathrm{e}^Y$ then the Baker-Campbell-Hausdorff formula says that this is equivalent to

$$\mathrm{e}^X \mathrm{e}^Y = \mathrm{e}^Z \tag{2.70}$$

with

$$Z = X + Y + \frac{1}{2}[X, Y] + \frac{1}{12}[X, [X, Y]] - \frac{1}{12}[Y, [X, Y]]... \tag{2.71}$$

We can use this to generate unitaries that are of arbitrary order as long as we have access to Gaussian unitaries and $e^{ic\hat{q}^3}$. So if we have a unitary generated by a monomial of order $M = m + n$ and a cubic phase gate, then the commutator between the monomial and $\hat{q}^3$ is

$$[\hat{q}^3, \hat{p}^m \hat{q}^n] = \mathrm{i}\hat{p}^{m-1}\hat{q}^{n+2} + \text{lower orders}. \tag{2.72}$$

Thus, as long as we have access to a Hamiltonian $\hat{q}^3$ and a monomial of order M, we can construct a monomial of order $M + 1$. We can build any polynomial of order $M + 1$ using Gaussian unitaries from this.

In the following, we will review the non-Gaussian states considered in this thesis.

Photon-added and -subtracted squeezed states Photon-added and photon-subtracted squeezed states [82] are widely used states due to their availability in optical systems. Theoretically, all bosonic quantum states can be created by combining photon addition [83] or subtractions [84] with linear operations. We define the L-photon-added or

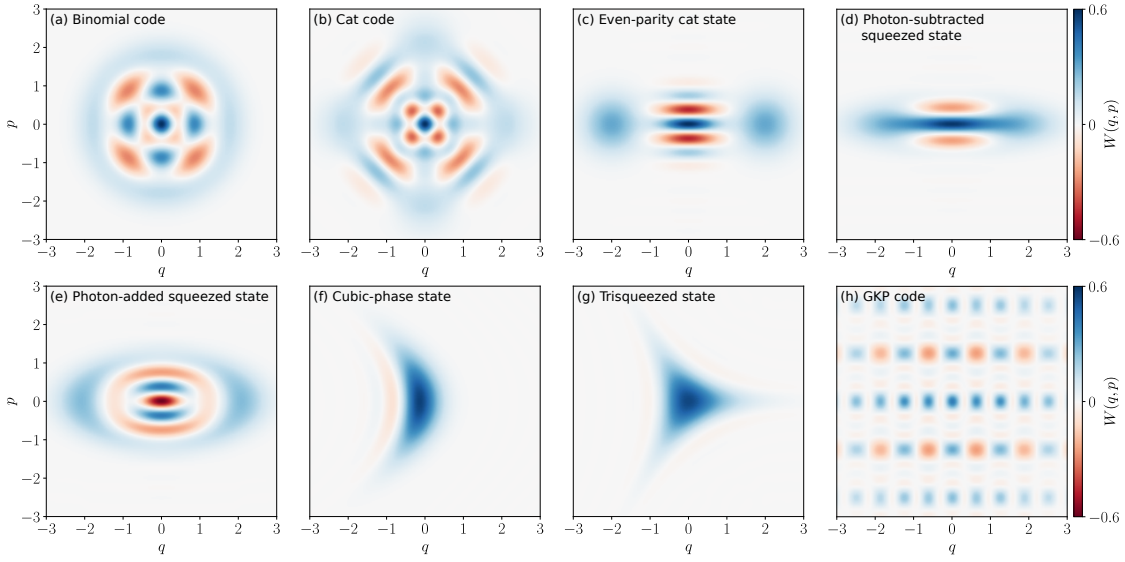

Figure 2.4: A collection of Wigner functions of the states we are considering. The color bar indicates the Wigner positivity (blue) and negativity (red) of the Wigner function $W(q,p)$ in normalized units. (a) Binomial code with rotation symmetry $N = 2$, truncation $K = 3$, and logical encoding $\mu = 0$. (b) Cat code with displacement $\alpha = 2$, $\mu = 0$, $N = 2$ and $r = \phi = 0$. (c) Even-parity cat state with displacement $\alpha = 2$. (d) Photon-subtracted squeezed state with $L = -2$ photons and squeezing $\xi = 5$ dB. (e) Photon-added squeezed state with $L = +3$ photons and squeezing $\xi = 3$ dB. (f) Cubic-phase state with cubicity $c = 0.551$ and squeezing -5 dB. (g) trisqueezed state, with triplicity $t = 0.1$. (h) GKP code with 14 dB squeezing, and for the code word $\mu = 0$.

-subtracted squeezed (PASS) state as ($L \in \mathbb{Z}$)

$$|\mathrm{PASS}_L\rangle = \begin{cases} \frac{1}{\mathcal{N}}\, \hat{a}^{|L|}\, |\alpha, \xi, \phi\rangle\,, & \text{if } L < 0, \\ \frac{1}{\mathcal{N}'}\, (\hat{a}^\dagger)^{|L|}\, |\alpha, \xi, \phi\rangle\,, & \text{if } L > 0, \end{cases} \tag{2.73}$$

where $\mathcal{N}$ and $\mathcal{N}'$ are normalizing constants. Photon-added and photon-subtracted squeezed states are widely used, especially for the generation of cat states [82], including recent proposals for direct generation of cat states that involve two input modes [85]. The Wigner functions of a photon subtracted and photon added squeezed state can be found in Fig. 2.4(d) and (e).

Cubic-phase state One of the most prominent non-Gaussian states is the cubic-phase state [25], shown in Fig. 2.4 (f). This state can be used to promote purely Gaussian operations to universality [80, 86] by implementing the cubic phase gate, as well as implementing the crucial non-Clifford T gate for GKP codes [25]. The cubic-phase state is defined as

$$|c\rangle = \mathrm{e}^{\mathrm{i}c\hat{q}^3}\, \hat{S}(\xi)\, |0\rangle\,, \tag{2.74}$$

where we refer to the parameter c as the *cubicity*. Due to its fundamental role in quantum information processing using continuous variables, various theoretical proposals have been put forward to generate such a state [16, 87–97], and recently a cubic-phase state was implemented experimentally in microwave cavities [98] as well as in optical systems [34].

trisqueezed State Another non-Gaussian resource state that has been experimentally implemented recently in a microwave architecture [99] is the trisqueezed state [100, 101], shown in Fig. 2.4 (g). The trisqueezed state is defined as

$$|t\rangle = \mathrm{e}^{\mathrm{i}(t^*\hat{a}^3 + t\hat{a}^{\dagger 3})}\, |0\rangle\,, \tag{2.75}$$

and we refer to the parameter t as its *triplicity*. As we will detail later, in Paper A , we developed a reliable Gaussian conversion protocol converting the trisqueezed state onto the cubic-phase state.

2.2.4 Bridging discrete and continuous-variable systems: Bosonic codes

The other type of universality describes the ability to encode discrete variables using bosonic codes in the infinite levels of the harmonic oscillators and then doing universal quantum computing in the code subspace. The two prominent families of bosonic codes differ in the type of symmetries they use to encode the quantum information.

Translationally symmetric bosonic codes: The GKP Code A family of states playing a significant role in this thesis is the Gottesman-Kitaev-Preskill (GKP) states [102]. They are a family of error correction codes that display translational symmetry. Thanks to this symmetry, this code was initially designed to protect against small shifts of the quadratures $\hat{q}, \hat{p}$. This thesis will also use this encoding to map magic and non-Gaussian resources.

In the following, we use a subscript to denote a continuous-variable state that encodes a discrete-variable state. For instance, $\hat{\rho}_{\mathrm{GKP}}$ refers to a continuous-variable state that encodes a qudit state $\hat{\rho}$ by the GKP encoding. The computational basis state $|j\rangle$ is encoded in the GKP code as an infinite superposition of position eigenstates as

$$|j\rangle_{\mathrm{GKP}} = \sum_{s=-\infty}^{\infty} \left|\hat{q} = \alpha(j + ds)\right\rangle, \tag{2.76}$$

A valuable property of the GKP code is that all Clifford unitaries on the code subspace can be implemented using Gaussian unitaries.

The ideal GKP state-like objects in Eq. (2.76) are non-normalizable and associated with infinite energy; thus, they are not proper quantum states or elements of the Hilbert space. We will still call them GKP states to have a readable text. To define physical GKP states with finite energy, we consider finitely squeezed GKP states [25, 103]

$$\left|\mu_{\kappa,\Delta}\right\rangle = \frac{1}{\sqrt{\mathcal{N}}} \sum_{s=-\infty}^{\infty} \mathrm{e}^{-\frac{1}{2}\kappa^2\alpha_d^2(ds+\mu)^2} \tag{2.77}$$

$$\times D\big(\alpha_d(ds+\mu)\big) S(-\log\Delta)\,|0\rangle \tag{2.78}$$

where $\mathcal{N}$ is a normalization constant, κ^{-1} is the width of the Gaussian envelope, Δ describes the individual squeezing parameter with $\log\big(\Delta^{-1}\big)$ and $\alpha_d = \sqrt{\frac{2\pi}{d}}$ a constant. One recovers the ideal GKP state with $\Delta, \kappa \to 0$. Fig. 2.4 (h) shows a Wigner plot of a GKP state.

Rotationally symmetric bosonic (RSB) codes A way to fault-tolerantly encode quantum information into bosonic systems consists of using rotation-symmetric codes [35]. RSB codes protect against photon loss, photon gain, and dephasing errors [35, 104]. These codes are characterized by the order N of rotation symmetry and normalized primitive states $|\Theta\rangle$. An order N-symmetric rotation code has the logical Z operator

$$\hat{Z}_N = \mathrm{e}^{\mathrm{i}(\pi/N)\hat{n}}. \tag{2.79}$$

The code words, i.e., the basis states which encode the 0 and 1 logical information in this case, are defined as

$$\left|\mu^N_{\mathrm{Rot}}\right\rangle = \frac{1}{\sqrt{\mathcal{N}}} \sum_{m=0}^{2N-1} (-1)^{\mu\cdot m} \mathrm{e}^{\mathrm{i}\frac{m\pi}{N}\hat{n}}\,|\Theta\rangle\,. \tag{2.80}$$

The primitive state $|\Theta\rangle$ has to have non-vanishing support on some even and odd Fock numbers. Cat and binomial codes are examples of rotationally symmetric bosonic codes [35].

Binomial codes are easier to define in the conjugate basis, where they are expressed as

$$\left|+_{\text{bin}}^{N,K}\right\rangle = \sum_{k=0}^{K} \sqrt{\frac{1}{2^K}\binom{K}{k}}\,|kN\rangle\,,$$
$$\left|-_{\text{bin}}^{N,K}\right\rangle = \sum_{k=0}^{K} (-1)^k \sqrt{\frac{1}{2^K}\binom{K}{k}}\,|kN\rangle\,. \tag{2.81}$$

Binomial codes with $N = 2$ and $K = 2$ have been demonstrated experimentally [98, 105].

For the case of cat-codes $\left|\mu_{\text{cat}}^{N,\alpha}\right\rangle$, the primitive state that one considers are coherent states$|\alpha\rangle = \hat{D}(\boldsymbol{\alpha})$

$$|\Theta_{\text{cat}}\rangle = |\alpha, r = 0, \phi = 0\rangle = |\alpha\rangle\,. \tag{2.82}$$

Note that in this thesis, we will use the term "cat states" to indicate the code words of a cat code with rotational symmetry of $N = 1$, see [35]. In particular, the code-words corresponding to $\mu = 0$ yields the even-parity cat state $\propto |\alpha\rangle + |-\alpha\rangle$ while $\mu = 1$ yields the even parity cat state $\propto |\alpha\rangle - |-\alpha\rangle$. Cat codes with $\alpha \simeq \sqrt{2}$ and $N = 2$ have been observed in experiments [98, 106, 107].

Figures 2.4 (a) and (b) show Wigner plots of binomial and cat codes, respectively, and (c) shows an even-parity cat state.

Squeezing convention

In this part of the thesis, we report how to convert different squeezing conventions. We hope it will be useful. To remind ourselves, we use the convention given in Eq.(2.27)

$$[\hat{q}, \hat{p}] = \mathrm{i}. \tag{2.83}$$

The squeezing operator is defined as

$$\hat{S}(\xi) = \mathrm{e}^{-\frac{\xi}{2}\hat{a}^{\dagger 2} + \frac{\xi^*}{2}\hat{a}^2} \tag{2.84}$$

with $\xi = r^{i\phi}$. The squeezing operator transforms annihilation and creation operators as

$$\hat{S}^\dagger(\xi)\hat{a}\hat{S}(\xi) = \hat{a}\cosh r - \hat{a}^\dagger \mathrm{e}^{\mathrm{i}\phi}\sinh r \tag{2.85}$$
$$\hat{S}^\dagger(\xi)\hat{a}^\dagger\hat{S}(\xi) = \hat{a}^\dagger\cosh r - \hat{a}\mathrm{e}^{-\mathrm{i}\phi}\sinh r. \tag{2.86}$$

For a general quadrature $\hat{q}_\lambda = \frac{1}{\sqrt{2}}(\hat{a}\mathrm{e}^{-\mathrm{i}\lambda} + \hat{a}^\dagger \mathrm{e}^{\mathrm{i}\lambda})$, the expectation value of $\hat{q}_\lambda^2$ is

$$\langle \xi | \hat{q}_\lambda^2 | \xi \rangle = \frac{1}{2}\left(\mathrm{e}^{2r} \sin\lambda - \frac{\phi}{2}^2 + \mathrm{e}^{-2r} \cos\lambda - \frac{\phi}{2}^2 \right). \tag{2.87}$$

Thus for real squeezing $\phi = 0$ and $\lambda = 0$, we obtain

$$\langle \xi | \hat{q}^2 | \xi \rangle = \frac{1}{2}\mathrm{e}^{-2r}. \tag{2.88}$$

The dB scale for squeezing is defined as

$$\mathrm{dB} = 10 \log_{10}\left(\frac{\Delta q^2}{\Delta q_0^2} \right) \tag{2.89}$$

where $\Delta q_0^2 = \frac{1}{2}$ is the variance of the vacuum state. Since $\langle \hat{q}_\lambda \rangle = 0$, we have the following translations

$$\mathrm{dB} = 10 \log_{10}\left(\mathrm{e}^{-2r} \right) \tag{2.90}$$

$$r = -\ln 10^{\frac{\mathrm{dB}}{20}}. \tag{2.91}$$

Chapter 3

Resource theories

In this chapter, we briefly review resource theories and refer the reader to [49, 108] for further details. Controlling quantum phenomena in an experiment to perform information processing tasks is the objective of intense study [109–111]. Many quantum phenomena are desirable properties that allow one to perform tasks that are impossible using classical means. A standard example is using entanglement to do quantum teleportation [112]. This led to treating quantum phenomena as resources used to perform specific tasks. The value of the resource is determined by its difficulty in being prepared experimentally and the usefulness it provides. In this framework, for instance, we say that entanglement is a resource for a communication task called quantum teleportation. However, many more tasks in quantum information processing require access to resourceful quantum states or operations or, in other words, use some quantum phenomena [108, 113]. Resource theories were introduced to study such quantum phenomena in quantum information theory. The basic idea behind resource theories is to perform quantum information processing with restricted operations. The quantum phenomenon or resource is not freely available or contained in the restricted set. Since quantum phenomena are the basis of resources in quantum resource theories, the restricted set is, in some sense, classical, while the resource allows unlocks very often quantumness. The restricted set plus resources always unlock the full power enabled by performing the task with quantum mechanical means. In some resource theories, the resource content is directly connected to the (exponential) classical simulation cost. We will see examples of this later in this thesis. We will start with technical definitions and then discuss the resource theory of magic and the resource theory of Wigner negativity in more detail.

3.1 Basic definitions

A resource theory is characterized by a set of free states $\mathcal{G}$ and a set of free operations $\mathcal{F}$. The set of free states is closed under the action of free operations. Namely, it holds for $\forall g \in \mathcal{G}$ that $\Lambda(g) \in \mathcal{G}, \forall \Lambda \in \mathcal{F}$. Every state not contained in the set of free states $\mathcal{G}$ is called a *resource*. Resource monotones have been introduced to quantify the resource content of a state and are defined as follows:

Definition 4 (Resource monotone)**.** *A mapping $\mathcal{M}$ from the set of all states to the real numbers is called a resource monotone if it is non-increasing under the set of free operations $\mathcal{F}$. It holds that for all states, i.e. $\forall \hat{\rho} \in \mathcal{H}$*

$$\mathcal{M}(\hat{\rho}) \geq \mathcal{M}(\Lambda(\hat{\rho})), \quad \forall \Lambda \in \mathcal{F} \tag{3.1}$$

Monotones in the literature do not necessarily fulfill all properties listed below, but the properties are helpful in their own right and will be used in this thesis.

Definition 5 (Faithfulness)**.** *A monotone is called faithful if there is a constant $c \in \mathbb{R}$ such that $\mathcal{M}(\hat{\rho}) = c, \forall \hat{\rho} \in \mathcal{G}$ and $\mathcal{M}(\hat{\rho}) > c$ otherwise.*

The most common conventions is either $c = 0$ if the monotone is (sub-)additive and $c = 1$ if the monotone is (sub-)multiplicative.

Definition 6 (Additivity and sub-additivity/ Multiplicativity and sub-multiplicativity)**.** *A monotone $\mathcal{M}$ is called additive if*

$$\mathcal{M}(\hat{\rho} \otimes \hat{\sigma}) = \mathcal{M}(\hat{\rho}) + \mathcal{M}(\hat{\sigma}) \tag{3.2}$$

A monotone $\mathcal{M}$ is called sub-additive if

$$\mathcal{M}(\hat{\rho} \otimes \hat{\sigma}) \leq \mathcal{M}(\hat{\rho}) + \mathcal{M}(\hat{\sigma}) \tag{3.3}$$

The same definitions hold if we replace addition $+$ with multiplication $\cdot$. This property is then analogously called (sub-)multiplicativity.

(Sub-)additivity is a beneficial property since it ensures that preparing a free state in an auxiliary system does not increase the resource amount.

Another property monotones can display is convexity.

Definition 7 (Convexity)**.** *A monotone $\mathcal{M}$ is called convex if*

$$\mathcal{M}\left(\int \mathrm{d}\nu p(\nu)\hat{\rho}_\nu\right) \leq \int \mathrm{d}\nu p(\nu)\mathcal{M}(\hat{\rho}_\nu) \tag{3.4}$$

Convexity is helpful to prove many properties and results using resource monotones.

Definition 8 (Monotonicity on average (ideal))**.** *A monotone $\mathcal{M}$ is called monotone on average if for a free trace-preserving operation Λ and their representation in terms of free Kraus operators $\{\hat{K}_{\boldsymbol{\lambda}}\}$ it holds that*

$$\mathcal{M}(\hat{\rho}) \geq \int \mathrm{d}\boldsymbol{\lambda} p(\boldsymbol{\lambda}|\hat{\rho}) \mathcal{M}(\hat{\sigma}_{\boldsymbol{\lambda}}) \tag{3.5}$$

for $\hat{\sigma}_{\boldsymbol{\lambda}} = \frac{1}{p(\boldsymbol{\lambda}|\hat{\rho})} \hat{K}_{\boldsymbol{\lambda}} \hat{\rho} \hat{K}_{\boldsymbol{\lambda}}^{\dagger}$.

For practical purposes, it is useful to consider a finite discrete set of Kraus operators, which leads to the following property, using the same notations as in the previous definition:

Definition 9 (Monotonicity on average (operational))**.** *A monotone $\mathcal{M}$ is called monotone on average in the operational sense if*

$$\mathcal{M}(\hat{\rho}) \geq \sum_i p_{i|\hat{\rho}} \mathcal{M}(\hat{\sigma}_i) \tag{3.6}$$

for $\hat{\sigma}_i = \frac{1}{p_{i|\rho}} \hat{K}_i \hat{\rho} \hat{K}_i^{\dagger}$.

Monotonicity (on average) allows for the investigation of probabilistic operations. This is an important property, especially when considering quantum optics, where genuine non-Gaussianity is usually generated probabilistically. A monotone with the property of monotonicity on average allows us to compute bounds, including bounds valid for probabilistic protocols. Indeed, given a resource monotone $\mathcal{M}$, if Λ is a free operation that maps k copies of $\hat{\rho}$ to m copies of $\hat{\sigma}$ with probability p, then monotonicity on average implies:

$$\mathcal{M}(\hat{\rho}^{\otimes k}) \geq p\, \mathcal{M}(\hat{\sigma}^{\otimes m}). \tag{3.7}$$

In case of an additive monotone, this reads

$$k\mathcal{M}(\hat{\rho}) \geq pm\, \mathcal{M}(\hat{\sigma}). \tag{3.8}$$

This bound can be seen as a constraint on the minimal number of copies of state $\hat{\rho}$ that need to be used if we wish to generate m copies of state $\hat{\sigma}$ with probability p.

In the case of monotones $\mathcal{M}$ that are only defined for pure state $|\psi\rangle\langle\psi|$, we can use a convex roof construction to generalize such monotone to mixed states [108]:

Definition 10 (Convex roof)**.** *Let $\mathcal{M}$ be a resource monotone that is only defined for pure states. This monotone can be extended to mixed states by the following convex roof extension:*

$$\mathcal{M}^{\cup}(\hat{\rho}) = \inf \sum_i p_i \mathcal{M}(|\psi_i\rangle\langle\psi_i|) \tag{3.9}$$

where the infimum is taken over all convex decompositions

$$\hat{\rho} = \sum_i p_i \left|\psi_i\right\rangle\!\left\langle\psi_i\right|, \quad p_i \geq 0 \quad \sum_i p_i = 1 \tag{3.10}$$

with pure states $|\psi_i\rangle\langle\psi_i|$.

3.2 Resources in discrete-variable QC: Magic

The leading architectures of fault-tolerant quantum computers are based on stabilizer codes [6]. In this approach, certain operations are easy to implement and constitute a non-universal [7] set that is fault-tolerant by having a transversal implementation —such that these operations do not propagate errors within a code block [8]. The Eastin-Knill theorem states that only a non-universal set of gates can be implemented transversally for a given quantum error correction code. For the most commonly studied error correction code, like the $2d$ surface code, Clifford unitary operations have a transversal implementation and are thus natively fault-tolerant. The question is then how to implement a non-Clifford gate, i.e., a $T-$gate while limiting the error propagation. Various methods exist to overcome this problem; however, implementing a fault-tolerant non-stabilizer gate is typically very costly [11].

The most common way is to deterministically use a non-stabilizer or $magic$ state to teleport a non-Clifford gate to the logical input state. This teleportation circuit is only allowed to consist of Clifford unitaries and computational basis measurement, so one is not trapped in a paradoxical loop. Which gates can be implemented this way is connected to the so-called Clifford hierarchy. The $n+1$ level of the Clifford hierarchy is defined as $C_{n+1} \equiv \{\hat{U} | \hat{U}\hat{P}\hat{U}^\dagger \subseteq C_n, \forall \hat{P} \in C_1\}$, where C_1 is the Pauli group and C_2 the Clifford unitary operators. Although any circuit can have an equivalent teleportation gadget, C_3 gates can be implemented with the corresponding resource states and conditional operators in the Clifford group. In Fig. 3.1, we show the teleportation circuit implementing a $T-$gate using $H-$type magic states.

This way, instead of implementing a non-Clifford gate, one requires high-fidelity magic states. Magic state distillation [114] is used to produce such high-quality magic states since these states cannot be implemented fault-tolerantly due to the restrictions of what gates can be implemented natively in a fault-tolerant manner. This technique uses many noisy states to distill a high-fidelity magic state and implement a high-fidelity non-Clifford gate. In a fault-tolerant quantum computation, most gates and qudits will be used to generate high-fidelity magic states in so-called magic state factories. So, one can say magic states are resourceful states for fault-tolerant quantum computing.

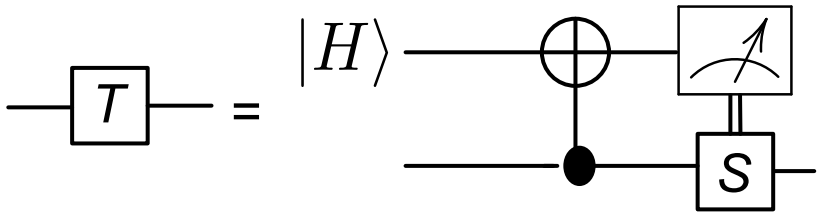

Figure 3.1: We can implement a $T-$gate using an $H-$type magic state. This state injection circuit teleports the $T-$gate using only Clifford unitaries, computational basis measurements, and feed-forward. Similar circuits can be constructed for all gates in the third level of the Clifford hierarchy, meaning they can be implemented using a magic state and Clifford unitaries computational with computational basis measurements.

Another reason to see Clifford operations as free operations lies in the Gottesman-Knill theorem [9]. This theorem holds for arbitrary discrete-variable systems, i.e., for all qudit dimensions:

Theorem 1 (Gottesman-Knill)**.** *Any quantum computer performing only: a) Clifford group gates, b) measurements of Pauli group operators, and c) Clifford group operations conditioned on classical bits, which may be the results of earlier measurements can be perfectly simulated in polynomial time on a probabilistic classical computer.*

Thus, stabilizer states and Clifford unitaries are insufficient to obtain exponential quantum advantage.

There is a very powerful magic monotone for odd-dimensional qudits, the negativity of the Wigner function [58]

Definition 11 (discrete Wigner negativity)**.** *For odd-dimensional systems, the discrete Wigner negativity is defined as*

$$\|W_{\hat{\rho}}^{\mathrm{DV}}\|_1 = \sum_{\boldsymbol{u}\in\mathbb{Z}_d^{2n}} \left|W_{\hat{\rho}}^{\mathrm{DV}}(\boldsymbol{u})\right|. \tag{3.11}$$

As we have seen in Sec. 2.1, the discrete Wigner function is a quasi-probability distribution and therefore can have negative values, but it is still normalized $\sum_{\boldsymbol{u}\in\mathbb{Z}_d^{2n}} W_{\hat{\rho}}^{\mathrm{DV}}(\boldsymbol{u}) = 1$. So, by instead summing up the absolute values, we can see how negative the discrete Wigner function is. The discrete Hudson's theorem states [56] that all pure stabilizer states are fully non-negative. The stabilizer protocols are the set of free operations under which the Wigner negativity is monotonic.

Definition 12 (Stabilizer Protocol)**.** *A stabilizer protocol is any map from $\hat{\rho} \in \mathcal{H}$ to $\hat{\sigma} \in \mathcal{H}'$ composed of the following operations*

- *Clifford unitaries: $\hat{\rho} \mapsto \hat{U}_C \hat{\rho} \hat{U}_C^\dagger$*
- *Composition with pure Stabilizer state: $\hat{\rho} \mapsto \hat{\rho} \otimes |\psi_S\rangle\langle\psi_S|$.*
- *Computational basis measurement of subsystem: $\hat{\rho} \mapsto (\mathbb{1} \otimes |i\rangle\langle i|)\hat{\rho}(\mathbb{1} \otimes |i\rangle\langle i|)/p(i|\hat{\rho})$, where $p(i|\hat{\rho}) = \mathrm{Tr}\big[\hat{\rho}(\mathbb{1} \otimes |i\rangle\langle i|)\big]$.*
- *Partial trace on subsystem: $\hat{\rho} \mapsto \mathrm{Tr}_B[\hat{\rho}]$.*
- *The above operations conditioned on*
  - *classical randomness*
  - *single measurement outcomes;*

The Wigner negativity is a faithful monotone with $\|W^{\mathrm{DV}}_{\hat{\rho}_S}\|_1 = 1$ for all stabilizer state $\hat{\rho}_S$ and is multiplicative $\|W^{\mathrm{DV}}_{\hat{\rho}\otimes\hat{\sigma}}\|_1 = \|W^{\mathrm{DV}}_{\hat{\rho}}\|_1 \|W^{\mathrm{DV}}_{\hat{\sigma}}\|_1$. The Wigner negativity is directly connected to the computational cost of simulating a quantum circuit through the simulator by Pashayan $et.\ al$ [115].

The story is not as simple for qubits or, more generally, even dimensional systems. Indeed, for even-dimensional systems, there is not one magic monotone that unifies many desirable properties. The mathematical structure of even-dimensional phase spaces, for example, the lack of multiplicative inverses (2^{-1}), prohibits a similar easy definition of a Wigner function. Even though it is possible to define one, it involves optimization over an over-complete basis, the closed and non-contextual sets consisting of stabilizer states [63, 64]. Doing that, one loses the property of multiplicativity of the Wigner function, leading to a restriction of a few qudits due to the optimization over the over-complete basis. Two very important magic monotones for qubits with a wide range of applications are the robustness of magic [44] and the stabilizer extent [43, 45], defined below:

Definition 13 (Robustness of magic)**.** *Given a density operator $\hat{\rho} \in \mathcal{H}$ — a n-qubit state—, the robustness of magic is defined as*

$$\mathcal{R}(\hat{\rho}) = \min_x \{\|x\|_1 = \sum_i |x_i|; \hat{\rho} = \sum_i x_i \hat{\sigma}_i\} \tag{3.12}$$

where $\hat{\sigma}_i$ are pure stabilizer states.

Definition 14 (Stabilizer extend)**.** *Given a pure state $|\psi\rangle \in \mathcal{H}$ — a n-qubit state—, the stabilizer extend is defined as*

$$\xi(|\psi\rangle) = \min_c \{\|c\|_1 = \sum_i |c_i|; |\psi\rangle = \sum_i x_i |\phi_i\rangle\} \tag{3.13}$$

where $|\phi_i\rangle$ are pure stabilizer states.

The robustness of magic and the stabilizer extent with the mixed state versions of the stabilizer extent — the dyadic negativity and the generalized robustness of magic— are monotonic under stabilizer protocols and faithful, but they have two significant drawbacks. They are sub-multiplicative and challenging to compute in general, which makes investigating larger systems computationally prohibitive. The robustness of magic and the stabilizer extent have a classical simulation algorithm associated with them. The runtime of these algorithms scales with the resource content quantified with the respective monotones.

Therefore, finding a magic monotone that is monotonic under stabilizer protocols, not prohibitively hard to compute, and quantifies the classical simulation cost would be desirable. We will address this question in Chap. 5, where we will define a magic measure to qudits that is easier to compute and connect it to simulation cost.

3.3 Resources in continuous-variable QC: Wigner negativity

As mentioned, Gaussian states and operations are essential in continuous-variable quantum information. Aside from the analytical methods available to study it, Gaussian quantum optics is readily available on many platforms. Quantum optics is the most apparent platform where Gaussian states and operations can be implemented relatively easily. However, Gaussian quantum optics is insufficient for quantum computing and other desired tasks. Therefore, one needs some form of non-Gaussianity. However, given our definition of Gaussian states, some non-Gaussian states and operations are easy to implement and not "useful." Probabilistic mixtures of Gaussian states can be non-Gaussian since the set of Gaussian states is non-convex. This notion is, however, more problematic to defend from an operational standpoint since generating one Gaussian state or the other based on a dice does not seem very resourceful. It is thus natural to use the convex hull of Gaussian states, i.e., convex mixtures of Gaussian states, as the set of free states. These states all have a positive Wigner function, making the negativity of the Wigner function a sign of genuine non-Gaussianity. We show the Wigner function of the vacuum state $|0\rangle$ and of the Fock state $|1\rangle$ in Fig. 3.2 to illustrate that. This genuine non-Gaussianity is, therefore, of interest for quantum computing using continuous variables. This can be seen as well from the following theorem [26, 54]:

Theorem 2 (Mari-Veitch (informal))**.** *Any quantum computer consisting only of states, gates, or, more generally, quantum channels and POVMs with positive Wigner functions can be efficiently simulated classically.*

Thus, we need Wigner negativity to have any chance of gaining a quantum advantage.

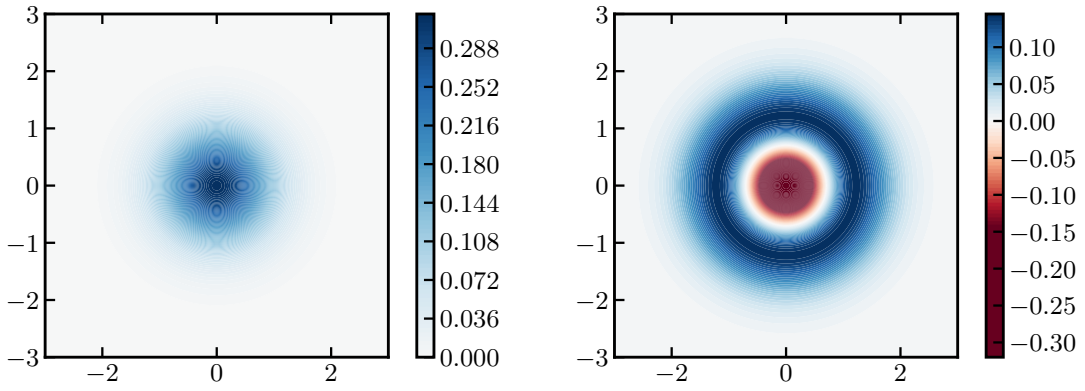

Figure 3.2: In the left panel, we show the Wigner function of a vacuum state $|0\rangle$, which is a Gaussian state, and on the right panel, The Wigner function of a Fock state $|1\rangle$. The vacuum state $|0\rangle$ is positive everywhere, while the non-Gaussian Fock state has a negative part in the middle.

A monotone of this resource theory of genuine non-Gaussianity is the continuous Wigner negativity.

Definition 15 (continuous Wigner negativity)**.** *The continuous Wigner negativity is defined as*

$$\|W_{\hat{\rho}}^{\mathrm{CV}}\|_1 = \int_{\mathbb{R}^{2n}} \mathrm{d}\boldsymbol{r} |W_{\hat{\rho}}(\boldsymbol{r})|. \tag{3.14}$$

Often, people use the logarithmic Wigner negativity, which is then defined as

$$\log \|W_{\hat{\rho}}^{\mathrm{CV}}\|_1 = \log \left(\int_{\mathbb{R}^{2n}} \mathrm{d}\boldsymbol{r} |W_{\hat{\rho}}({}^{\mathrm{CV}}\boldsymbol{r})| \right). \tag{3.15}$$

The set of free operations for the continuous Wigner negativity are the Gaussian protocols. We define Gaussian protocols as follows [49]:

Definition 16 (Gaussian Protocol)**.** *A Gaussian protocol is a map from $\hat{\rho} \in \mathcal{H}$ to $\hat{\sigma} \in \mathcal{H}'$ composed of the following operations*

- *Gaussian unitaries: $\hat{\rho} \mapsto \hat{U}_G \hat{\rho} \hat{U}_G^\dagger$*
- *Composition with pure Gaussian state: $\hat{\rho} \mapsto \hat{\rho} \otimes |\psi_G\rangle\langle\psi_G|$.*
- *Pure Gaussian measurement of subsystem: $\hat{\rho} \mapsto \mathrm{Tr}_B[\hat{\rho}(\mathbb{1} \otimes |\psi_G(\boldsymbol{\alpha})\rangle\langle\psi_G(\boldsymbol{\alpha})|)]/p(\boldsymbol{\alpha}|\hat{\rho})$, where $p(\boldsymbol{\alpha}|\hat{\rho}) = \mathrm{Tr}\left[\hat{\rho}(\mathbb{1} \otimes |\psi_G(\boldsymbol{\alpha})\rangle\langle\psi_G(\boldsymbol{\alpha})|)\right]$ and $\boldsymbol{\alpha}$ a vector of real measurement outcomes.*

- *Partial trace on subsystem:* $\hat{\rho} \mapsto \mathrm{Tr}_B[\hat{\rho}]$.
- *The above operations conditioned on*
  - *classical randomness;*
  - *single measurement outcomes (ideal case);*
  - *measurement outcomes falling into finite-size intervals (operational case).*

The Wigner negativity is a faithful monotone with $\|W^{\mathrm{CV}}_{\hat{\rho}_G}\|_1$=1 for ρ_G Gaussian states or, more generally, Wigner positive states, including the convex hull of Gaussian states. It is multiplicative (additive for the logarithmic Wigner negativity).

Chapter 4

Conversion protocols for continuous-variable quantum computing

In this chapter, we will discuss the Gaussian conversion protocols. We used these to study conversions in Paper Aand Paper C. Non-Gaussian states are challenging to generate. In quantum optics, their generation is mostly probabilistic, and many experimental setups are limited in what states can be generated. So, if we have a non-Gaussian state but want a different non-Gaussian state to perform a specific task, can we use Gaussian and thus free operations? The resource theory of genuine non-Gaussianty developed so far [48, 49] provides bounds on these conversions, but what if we are interested not in exact conversion but only in approximate conversion, up to a (possibly high) fidelity between the output state of the conversion and the target state? Current non-Gaussian monotones do not allow us to bound approximate conversions, i.e., to consider conversions that do not yield fidelity $= 1$. Furthermore, in some scenarios, we want to restrict conversions to deterministic ones since the generation of the target state is often already probabilistic. One may, for example, not want to further reduce the success probability.

4.1 Deterministic conversion protocols

To study the Gaussian deterministic protocols, we will use Gaussian CPTP maps to transform an input state, the state we have available, into a target state, the state we want. We design a CPTP map so that the fidelity between the output state and the target state is maximized. We will use the characteristic function formalism because it allows for a useful characterization of Gaussian CPTP maps. For convenience, we will repeat the characterization here from Sec. 2.2. The action of any Gaussian CPTP-map Φ on

the characteristic function can then be written as [71]:

$$\chi_{\hat{\rho}}(\boldsymbol{r}) \rightarrow \chi_{\Phi(\hat{\rho})}(\boldsymbol{r}) = \mathrm{e}^{-\frac{1}{4}\boldsymbol{r}^T\Omega^T Y\Omega\boldsymbol{r}+\mathrm{i}\boldsymbol{l}^T\Omega\boldsymbol{r}}\chi_{\hat{\rho}}(\Omega^T X^T\Omega\boldsymbol{r}) \tag{4.1}$$

with X,Y being $2N \times 2N$ real matrices, $\boldsymbol{l}$ being a $2N$ real vector, Y being symmetric, and fulfilling the following positive semi-definite matrix constraint:

$$Y \pm \mathrm{i}(\Omega - X\Omega X^T) \geq 0 \; . \tag{4.2}$$

Notice that Eq. (2.67), in turn, implies that Y has to be a positive semi-definite matrix. $\boldsymbol{l}$ characterizes the displacement on the state; Y denotes the action of Gaussian auxiliary systems, and X the reduced action of a general Gaussian unitary on all the modes, including the Gaussian auxiliary modes on the input state. To study the conversion between an input and target state, we will transform the input state using the Gaussian CPTP map from Eq. (2.66) and numerically maximize the fidelity of the transformed state and the target state by numerically finding the optimal parameters $X, Y, \boldsymbol{l}$ fulfilling the constraints Eq. (2.67). Note that the Gaussian CPTP maps are generally non-constructive; we cannot immediately know how to implement them in the lab. The reason is the addition of an unspecified number of Gaussian auxiliary states.

We start by noting that for speeding up the numerical calculation of the characteristic function, it is useful to rewrite the characteristic function using the Fock state basis as

$$\chi_{\hat{\rho}}(\boldsymbol{r}) = \mathrm{Tr}\Big\{\hat{D}(-\boldsymbol{r})\hat{\rho}\Big\} = \sum_{n,m=0}^{\infty} \rho_{nm} \left\langle m\right| \hat{D}(-\boldsymbol{r}) \left|n\right\rangle . \tag{4.3}$$

The matrix elements of the displacement operator appearing at the RHS of Eq. (4.3) can now be written for $m \geq n$ as [116]

$$\left\langle m\right| \hat{D}(\alpha) \left|n\right\rangle = \sqrt{\frac{n!}{m!}}\mathrm{e}^{-|\alpha|^2/2}\alpha^{m-n}L_n^{m-n}(|\alpha|^2) \tag{4.4}$$

and for $m \leq n$

$$\left\langle m\right| \hat{D}(\alpha) \left|n\right\rangle = \sqrt{\frac{m!}{n!}}\mathrm{e}^{-|\alpha|^2/2}(-\alpha^*)^{m-n}L_m^{n-m}(|\alpha|^2), \tag{4.5}$$

where $L_m^{n-m}(|\alpha|^2)$ are the associated Laguerre polynomials. Using the Laguerre polynomials instead of numerically evaluating $\mathrm{Tr}\Big\{\hat{D}(-\boldsymbol{r})\hat{\rho}\Big\}$ greatly speeds up the numerical evaluation.

To further improve the numerical performance, we can simplify the constraints (2.67) for a single mode.

For a matrix to be positive-semidefinite, the eigenvalues $\lambda_{1,2}$ satisfy the constraint $\lambda_{1,2} \geq 0$. We rewrite the constraint Eq. (2.67) as

$$Y \pm \mathrm{i}(1 - \det(X))\Omega \geq 0 \tag{4.6}$$

$$\lambda_{1,2} = \frac{1}{2}\left(Y_{11} + Y_{22} \pm \sqrt{(Y_{11} + Y_{22})^2 - 4\Big(Y_{11}Y_{22} - (Y_{12} \pm \mathrm{i}\tilde{X})(Y_{21} \mp \mathrm{i}\tilde{X})\Big)}\right) \tag{4.7}$$

$$= \frac{1}{2}\left(Y_{11} + Y_{22} \pm \sqrt{(Y_{11} + Y_{22})^2 - 4\Big(Y_{11}Y_{22} - Y_{12}Y_{21} - \tilde{X}^2 \pm \mathrm{i}\tilde{X}Y_{12} \mp \mathrm{i}\tilde{X}Y_{21}\Big)}\right) \geq 0 \tag{4.8}$$

where $\tilde{X} = (1 - \det(X))$ and $\lambda_{1,2} = \frac{1}{2}\left(\mathrm{Tr}(A) \pm \sqrt{\mathrm{Tr}(A)^2 - 4\det(A)}\right)$. Then, we can simplify the inequality by only considering the minus sign and remembering that Y is symmetric, obtaining

$$Y_{11} + Y_{22} \geq \sqrt{(Y_{11} + Y_{22})^2 - 4\Big(Y_{11}Y_{22} - Y_{12}Y_{21} - \tilde{X}^2\Big)} \tag{4.9}$$

We simplify this further by using that Y is positive semi-definite

$$(Y_{11} + Y_{22})^2 \geq (Y_{11} + Y_{22})^2 - 4\Big(Y_{11}Y_{22} - Y_{12}Y_{21} - \tilde{X}^2\Big) \tag{4.10}$$

$$\det(Y) \geq \tilde{X}^2. \tag{4.11}$$

This equation is simpler to evaluate numerically, so we can explore new optimization parameters faster to maximize the fidelity.

If the Y matrix consists of 0, the Gaussian CPTP map consists only of symplectic transformations and displacements. It is, therefore, unitary. For $Y = 0$, the constraint Eq. (2.67) is equivalent to demanding that X is a symplectic matrix. Using our simplified constraint for one mode, we immediately see that for $Y = 0$, we have $\det[X] = 1$, which is a sufficient condition for a 2×2 matrix to be symplectic. Since we know that $X \in \mathrm{Sp}(2, \mathbb{R})$, we can parameterize the transformation using the following parametrization [72]:

$$X = \begin{pmatrix} g & ge \\ cg & g^{-1} + cge \end{pmatrix}, \tag{4.12}$$

for $g, e, c \in \mathbb{R}$ and non-zero g. In other words, we are using 3 real parameters to parameterize a real symplectic transformation, which is precisely the dimension of the real symplectic group $\mathrm{Sp}(2, \mathbb{R})$. We use a second parametrization that uses the Euler decomposition (see Eq. (2.45) for the operator version). Every symplectic transformation can

be decomposed as [71]

$$S = U_L Z V_L, \tag{4.13}$$

$$Z = \bigoplus_{i=1}^{n} \begin{pmatrix} z_i & 0 \\ 0 & z_i^{-1} \end{pmatrix}, \tag{4.14}$$

where U_L, V_L are passive symplectic transformation $U_L, V_L \in \mathrm{Sp}(2n, \mathbb{R}) \cap O(2n)$. The next section will discuss how to parameterize passive symplectic matrices.

4.1.1 Passive transformations

The group of passive symplectic transformations $K(n) = \mathrm{Sp}(2n, \mathbb{R}) \cap O(2n)$ is the compact subgroup of the symplectic group $\mathrm{Sp}(2n, \mathbb{R})$ and is isomorphic to $U(n)$. This means that n modes require n parameters. For comparison, the general symplectic group needs $2n + n$ parameters.

A passive symplectic matrix $S \in K(n)$ can be written as

$$S = \begin{pmatrix} X & Y \\ -Y & X \end{pmatrix} \tag{4.15}$$

for X, Y $n \times n$ matrices that fulfill the following constraints

$$XY^T - YX^T = 0 \tag{4.16}$$

$$XX^T + YY^T = 1. \tag{4.17}$$

We can rewrite these constraints if we use $U = X + \mathrm{i}Y$

$$UU^\dagger = XX^T + YY^T + \mathrm{i}(YX^T - XY^T) = 1. \tag{4.18}$$

We see that X and Y are the real and imaginary parts of a unitary matrix U. So we can write about the transformation

$$\bar{U} = \frac{1}{\sqrt{2}} \begin{pmatrix} \mathbb{1} & \mathrm{i}\mathbb{1} \\ \mathbb{1} & -\mathrm{i}\mathbb{1} \end{pmatrix} \tag{4.19}$$

that

$$\bar{U} \begin{pmatrix} X & Y \\ -Y & X \end{pmatrix} \bar{U}^\dagger = \begin{pmatrix} U^* & 0 \\ 0 & U \end{pmatrix}. \tag{4.20}$$

Note that $\bar{U}$ is the transformation that maps between the quadratures and the creation and annihilation operators $\hat{q}, \hat{p} \to \hat{a}, \hat{a}^\dagger$. So, we can use this to parameterize the passive symplectic matrix S. Note that for a single mode S is a 2×2 matrix, so U is a unitary 1×1 "matrix," which is just a phase $\mathrm{e}^{\mathrm{i}\phi}$. For more modes, we need to parameterize larger unitary matrices.

4.2 Results

4.2.1 Conversion of trisqueezed state to cubic phase state

The first conversion we study is from the trisqueezed to the cubic phase state. We studied this conversion in Paper A. The trisqueezed state has been implemented using superconducting circuits, however no direct use case in quantum information processing was known. The cubic phase state has many applications, mainly to allow for universal CV quantum computing by implementing non-Gaussian dynamics with Gaussian unitaries or being the $T-$gate on the logical subspace of a GKP state, as we have seen in Sec 2.2.

We defined the input trisqueezed state in Eq. (2.75) as

$$|\Psi_{\text{in}}\rangle = \mathrm{e}^{\mathrm{i}(t^*\hat{a}^3 + t\hat{a}^{\dagger 3})} |0\rangle . \tag{4.21}$$

The target finitely squeezed cubic phase state was defined in Eq. (2.74) as

$$\left|\Psi_{\text{target}}\right\rangle = \mathrm{e}^{\mathrm{i}c\hat{q}^3} \hat{S}(\xi_{\text{target}}) |0\rangle . \tag{4.22}$$

In the target cubic phase state, we fixed 5dB squeezing, or $\xi_{\text{target}} = -\log 10^{\frac{5}{20}}$, to reduce the degrees of freedom and pick a realistic value of squeezing.

First, we match the triplicity and cubicity of the input and target states so that they have the same continuous Wigner negativity. We do this so that we can, in principle, allow direct conversion with unity fidelity since Gaussian unitaries keep the Wigner negativity invariant.

We then optimize the parameters $X, Y, \boldsymbol{l}$ in Eq. (2.66) to maximize the fidelity of the transformed input state with a Gaussian CPTP map and the target state. During the numerical optimization, we saw that all optimal values involve setting Y to the matrix containing only 0. This is unsurprising since Y adds a Gaussian blur to the characteristic function. However, we are interested in converting a pure state to a pure state, making it unlikely that involving Gaussian noise increases the fidelity. Consequently, since $Y = 0$, the optimal protocol is a symplectic transformation consisting only of real squeezing plus displacement. The optimal fidelity for $t = 0.1$ and $c = 0.0551$ is $\mathcal{F} = 0.9708$. We can understand this simple transformation as follows. We denote the Gaussian unitary operation associated with the symplectic matrix X as $\hat{U}_X$. $\hat{U}_X$ then transforms the trisqueezed state as

$$\hat{U}_X \mathrm{e}^{\mathrm{i}t(\hat{a}^3 + \hat{a}^{\dagger 3})} |0\rangle = \hat{U}_X \mathrm{e}^{\mathrm{i}t(\hat{a}^3 + \hat{a}^{\dagger 3})} \hat{U}_X^\dagger \hat{U}_X |0\rangle . \tag{4.23}$$

For exact state conversion, the following has to hold:

$$\hat{U}_X \mathrm{e}^{\mathrm{i}t(\hat{a}^3 + \hat{a}^{\dagger 3})} \hat{U}_X^\dagger \to \mathrm{e}^{\mathrm{i}c\hat{q}^3}. \tag{4.24}$$

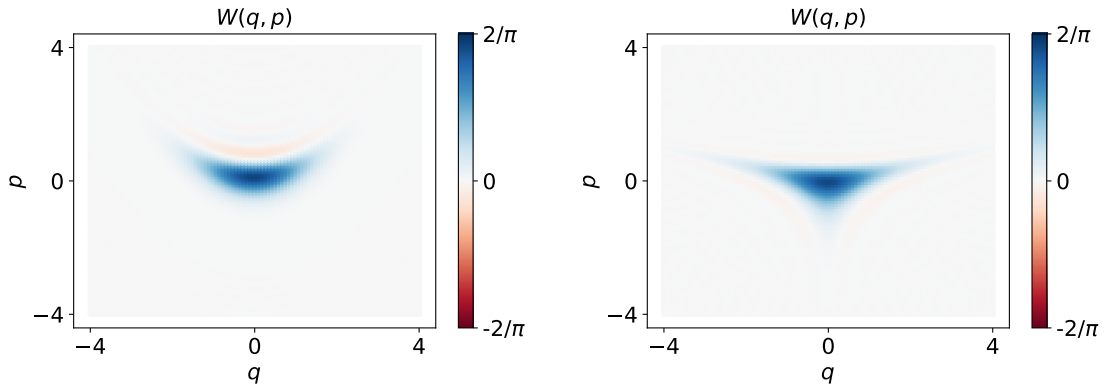

Figure 4.1: Displayed are the target state of our conversions protocol, which is a cubic phase state with $c = 0.0551$ and 5dB squeezing, and the output of the conversion protocol. If we compare the left and right panels, we see some differences in the features, for instance, a residual third "leg" of the output state, which is not present in the target cubic phase state. The fidelity with the target cubic phase state of $\mathcal{F} = 0.9708$ is fairly high.

This can be achieved asymptotically in the infinite squeezing limit. Squeezing implements the Bogoliubov transformation

$$\hat{a} \to \hat{S}(\xi)\hat{a}\hat{S}^\dagger(\xi) = u\hat{a} + v\hat{a}^\dagger \tag{4.25}$$

$$\hat{a}^\dagger \to \hat{S}(\xi)\hat{a}^\dagger\hat{S}^\dagger(\xi) = u^*\hat{a}^\dagger + v^*\hat{a} \tag{4.26}$$

with $u = \cosh(|\xi|)$ and $v = \sinh(|\xi|)\,\mathrm{e}^{-i\phi}$. In the case of $u = v$ and $u^* = v^*$, this transformation gives us the required form, because $\hat{q} \propto \hat{a} + \hat{a}^\dagger$. Thus, we can transform a trisqueezed state into a cubic phase state in the asymptotic limit $|\xi| \to \infty$ and $\phi = 0$. Therefore, the squeezing parameter ξ_{target} associated with the target cubic phase state is finite; one expects that the optimal squeezing operation will be a trade-off between matching the target state squeezing and transforming the trisqueezed state.

In Fig. 4.1, we show the Wigner function of the input and the maximized output of the Gaussian CPTP map. As we see in Fig. 4.1, although the fidelity is high, the features are not reproduced. By comparing the left and right panels, we observe that only one of the "legs" of the trisqueezed state is smaller but did not vanish completely. We need to do more to reproduce the cubic phase state feature better.

We extend our conversion toolbox and consider the following probabilistic protocol. The circuit that we are considering is shown in Fig. 4.2. We take the same trisqueezed state as our input state and prepare an additional Gaussian state with squeezing ξ and displacement β. We let them interact through a beamsplitter and then post-select the upper mode on $q = 0$ with an acceptance region $\pm\delta$. The acceptance region δ determines

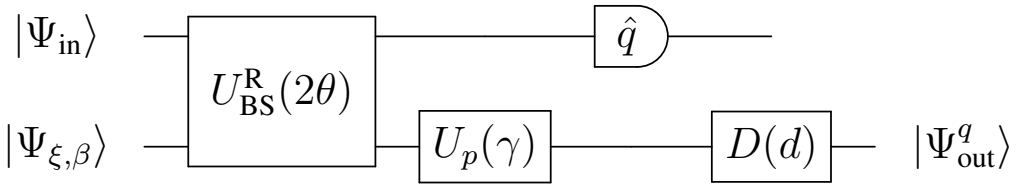

Figure 4.2: This is the circuit we are considering for our probabilistic protocol. On the top rail, we start with trisqueezed states as $|\Psi_{\text{in}}\rangle$, while on the bottom rail is a Gaussian state with squeezing ξ and displacement β. The two modes interact through a beamsplitter with real parameter θ. On the top mode, we measure $\hat{q}$ and post-select on the measurement outcome $q = 0 \pm \delta$, where δ describes the acceptance region. On the bottom mode, we will act with a rotation parameterized with γ and a displacement with d.

the acceptance probability of the protocol. Suppose $\delta = 0$, then the probability is $p = 0$ since we would be postselecting on a continuous value. We allow further rotations with angle γ and displacements d on the bottom mode. We then optimize the parameters $\xi, \beta, \gamma, \theta, d$ to maximize the fidelity of the output state with the target cubic phase state.

We obtain for the case of $t = 0.1$ and $c = 0.0551$ a very high fidelity $\mathcal{F} = 0.9971$ with a success probability of $p = 0.0513$. In this case, we reproduce the features correctly as well. In Fig. 4.3, we show the Wigner function of the output of the deterministic and the probabilistic protocol and the target cubic phase state along several lines in phase space. We see that the deterministic protocol cannot approximate some of the features of the target state, as seen in the bottom panels. The fidelity is still high since the features with the most weight are well approximated, as seen in the top panels. The probabilistic protocol, however, allows us to approximate the more intricate feature of the cubic phase state, as seen in the bottom panels.

For the reason mentioned above, we are interested in finding further deterministic protocols for conversion between relevant non-Gaussian states. Can we find a conversion between pure non-Gaussian states that uses deterministic Gaussian maps? This is the question we investigate in the following subsection.

4.2.2 Conversion of photon-added or photon-subtracted squeezed states to cat states

This subsection investigates more deterministic Gaussian conversion protocols between non-Gaussian states. These findings were published in Paper C. We used our numerically efficient code to scan many interesting quantum states. Based on numerical simu-

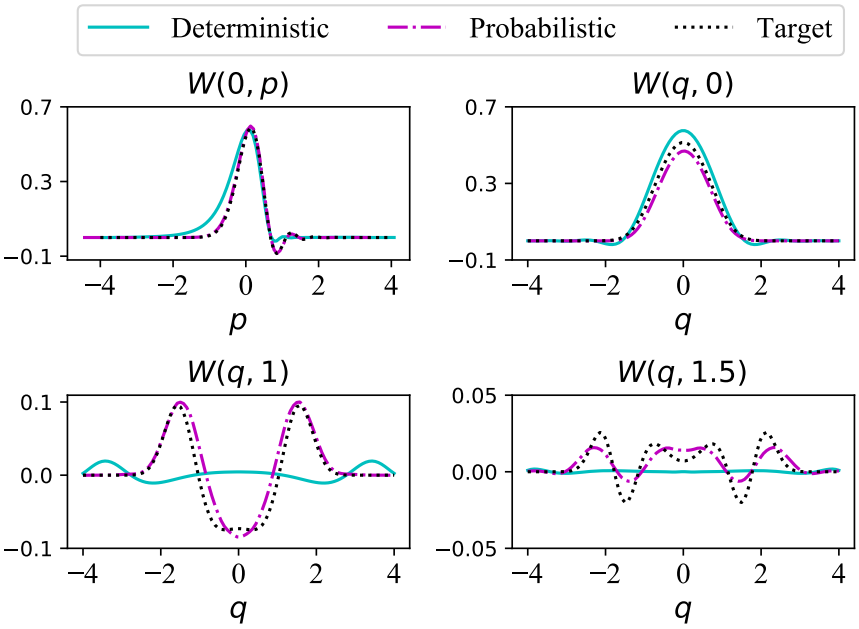

Figure 4.3: This figure shows cuts of the Wigner functions of the output state of the optimal deterministic and the probabilistic protocol in a trisqueezed state with $t = 0.1$ as well as the target cubic phase state with $c = 0.0551$ in phase space. On the top panels, we see that both protocols can approximate the target state fairly well; the probabilistic protocol, however, reproduced nearly the target Wigner function. On the bottom panels, we see that the deterministic protocol cannot reproduce the features of the target Wigner function on these lines in phase space. The probabilistic protocol instead allows for a good approximation of the target state.

lations, we conduct an exhaustive study of single-mode Gaussian conversions between non-Gaussian bosonic states.

An example we study is photon subtracted/added squeezed states to cat states. We defined in Eq. (2.73) the L-photon-added or -subtracted squeezed (PASS) state with($L \in \mathbb{Z}$) as our input states

$$|\mathrm{PASS}_L\rangle = \begin{cases} \frac{1}{\mathcal{N}}\, \hat{a}^{|L|}\, |\alpha, \xi, \phi\rangle\,, & \text{if } L < 0, \\ \frac{1}{\mathcal{N}'}\, (\hat{a}^\dagger)^{|L|}\, |\alpha, \xi, \phi\rangle\,, & \text{if } L > 0, \end{cases} \tag{4.27}$$

where $\mathcal{N}$ and $\mathcal{N}'$ are normalizing constants. The target states are the even/odd parity cat states

$$\left|\mathrm{cat}_\alpha^\pm\right\rangle = \frac{1}{\mathcal{N}}\big(|\alpha\rangle \pm |-\alpha\rangle\big) \tag{4.28}$$

with $\mathcal{N}$ a normalization constant. They are called even/odd parity because they only have support on even/odd Fock states. Cat states can be generated from photon added-subtracted squeezed states if $\alpha \leq 1$ [82, 117]. However, this generation technique presents considerable experimental challenges when cat states of larger amplitudes are targeted since the fidelity between the target and PASS states is high only for large numbers of photon additions/subtractions, which, in turn, implies complex optical networks and low generation probabilities [82].

We will discuss this conversion using an example. We choose an even cat state with amplitude $\alpha = 2$ as the target state. This scenario is shown in Fig. 4.4. With two-photon subtractions at disposal ($L = -2$), the best fidelity achievable without conversion is $F = 0.891$, obtained for a PASS state with $L = -2$ and $\xi = 0.7$. On the other hand, using our optimized conversion protocol (specifically, given by a squeezing operation of amount $\Xi = -1.06$), the value of $F = 0.95$ can be achieved using a PASS state with $L = -2$ and $\xi = 1.3$. With four-photon subtractions at disposal, the maximal fidelity achievable without conversion is given by $F = 0.95$, obtained for a PASS state with $L = -4$ and $\xi = 0.5$. Using a conversion protocol can improve this to $F = 0.995$, considering a PASS state with $L = -4$ and $\xi = 1$ and enacting on it with an additional squeezing of amount $\Xi = -1.16$. Namely, an almost perfect conversion can be attained even deterministically.

Even though we could improve the cat state generation from PASS and found a good conversion protocol between trisqueezed and cubic phase states, we could not identify good conversions between other relevant non-Gaussian states. We investigated many states over vast parameter regimes, but in the end, Gaussian deterministic protocols are too restricted. Therefore, it would be interesting to investigate Gaussian maps that are n to m modes with $n > m$, i.e., probabilistic protocols. This is now under investigation in our group.

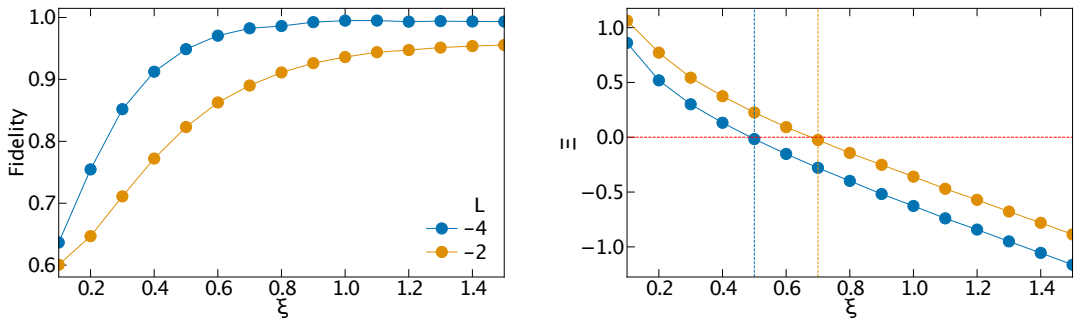

Figure 4.4: This figure shows the conversion between a PASS state with squeezing ξ and L photon subtractions and an even-parity cat state with $\alpha = 2$. The first panel shows the fidelities between the converted PASS state and the cat state, using a Gaussian CPTP. The Gaussian map is effectively only squeezing with strength Ξ. In the second panel, we plot the map's optimal squeezing of Ξ as a function of the input squeezing ξ of the PASS state. The vertical lines show the squeezing for which the PASS and cat states have maximal fidelity without any transformation. We can greatly improve cat state generation by applying additional Gaussian unitaries and photon addition and subtraction. For $L = -4$ subtractions, we can get nearly unital fidelity.

Chapter 5

Quantifying magic in discrete-variable systems

In this chapter, we will introduce new magic quantifiers for discrete-variable systems that are based on continuous-variable techniques. We formally show a direct connection between the resource theory of magic and the resource theory of genuine non-Gaussianity. Paper B discusses the case for qubits, while Paper D encapsulates all qudit dimensions and connects the new quantifiers to the cost of simulating a quantum circuit.

5.1 General approach

In the following, we use a subscript to denote a continuous-variable state that encodes a discrete-variable state. For instance, $\hat{\rho}_{\mathrm{GKP}}$ refers to a continuous-variable state that encodes a qudit state $\hat{\rho}$ by the GKP encoding. The computational basis state $|j\rangle$ of a qudit is encoded in the GKP code as an infinite superposition of position eigenstates as

$$|j\rangle_{\mathrm{GKP}} = \sum_{s=-\infty}^{\infty} \left|\hat{q} = \alpha(j + ds)\right\rangle . \tag{5.1}$$

Note that these code words are not normalizable quantum states, i.e., they are not elements of a Hilbert space. As mentioned, there are ways to define and use finite energy GKP states. However, we only require them as a mathematical tool, meaning we do not care that they are not normalizable. The Wigner function of a GKP code word is given

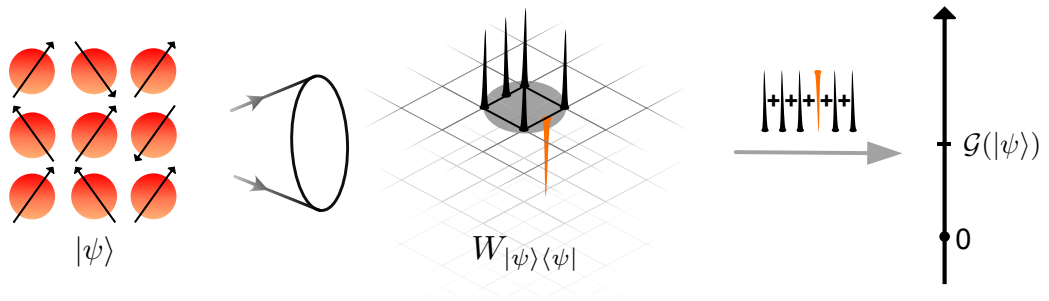

Figure 5.1: This sketch summarizes our approach to connecting discrete variables with continuous variables and the resource theory of magic with the resource theory of non-Gaussianity. We encode a DV state $|\psi\rangle$ in the continuous-variable GKP code. After the encoding, we compute the Wigner function and the Wigner negativity of the GKP state. We show that the renormalized Wigner negativity of the GKP state encoding a DV state $|\psi\rangle$ is a magic quantifier for all dimensions, directly connecting the resource content of a continuous-variable object in the resource theory of non-Gaussianty with the resource content of the encoded DV state in the resource theory of magic.

by [102]

$$W^{\mathrm{CV}}_{|j\rangle\langle j|_{\mathrm{GKP}}}(r_q, r_p) \propto \sum_{s,t=-\infty}^{\infty} (-1)^{st} \delta\left(r_p - \frac{\pi}{d\alpha} s\right) \delta\left(r_q - \alpha j - \frac{d\alpha}{2} t\right) \tag{5.2}$$

with $\alpha = \sqrt{\frac{2\pi}{d}}$. A valuable property of the GKP code that we will use is that all Clifford unitaries on the code subspace can be implemented using Gaussian unitaries.

Every GKP state that encodes a quantum state $\hat{\rho}$ can be brought into a form that we call "atomic form," where all Dirac distributions have disjoint support:

$$W^{\mathrm{CV}}_{\hat{\rho}_{\mathrm{GKP}}}(\boldsymbol{r}) = \frac{\sqrt{d}^n}{\sqrt{8\pi}^n} \sum_{\boldsymbol{l},\boldsymbol{m}} c_{\rho_{\mathrm{GKP}}}(\boldsymbol{l}, \boldsymbol{m}) \delta\left(\boldsymbol{r_p} - \boldsymbol{m}\sqrt{\frac{\pi}{2d}}\right) \delta\left(\boldsymbol{r_q} - \boldsymbol{l}\sqrt{\frac{\pi}{2d}}\right), \tag{5.3}$$

with $\boldsymbol{r} = (r_{q,1}, ..., r_{q,n}, r_{p,1}, ..., r_{p,n})$ and $\boldsymbol{l} = (l_1, ..., l_n)$, $\boldsymbol{m} = (m_1, ..., m_n)$. We are now interested in finding an explicit expression for the coefficients $c_{\rho_{\mathrm{GKP}}}(\boldsymbol{l}, \boldsymbol{m})$. We introduce a new operator basis for qudit systems to make this connection. For $l, m \in \mathbb{Z}_{2d}$, let $O_{l,m}$ be an operator defined by

$$\hat{O}_{l,m} = \omega_d^{-ml/2} \hat{M}_l \hat{Z}_d^m \tag{5.4}$$

where

$$\hat{M}_l = \sum_{\substack{u,v\in\mathbb{Z}_d \\ u+v \mod d=l}} |u\rangle\langle v| \tag{5.5}$$

and $\hat{Z}_d$ being the generalized Pauli Z operator and ω_d the dth root of unity. This can easily be extended to n-qudit systems, where we define $\hat{O}_{\boldsymbol{l},\boldsymbol{m}} = \bigotimes_{i=1}^{n} \hat{O}_{l_i,m_i}$ for $\boldsymbol{l},\boldsymbol{m} \in \mathbb{Z}_{2d}^n$. Using these operators, we show in Paper D the following connection. For $\boldsymbol{l},\boldsymbol{m} \in \mathbb{Z}_{2d}^n$, it holds that

$$c_{\rho_{\mathrm{GKP}}}(\boldsymbol{l},\boldsymbol{m}) = x_{\hat{\rho}}(\boldsymbol{l},\boldsymbol{m}), \tag{5.6}$$

where

$$x_{\hat{\rho}}(\boldsymbol{l},\boldsymbol{m}) \coloneqq d^{-n} \operatorname{Tr}\left(\hat{O}_{\boldsymbol{l},\boldsymbol{m}}\hat{\rho}\right) \tag{5.7}$$

which corresponds to the coefficients for $\hat{O}_{\boldsymbol{l},\boldsymbol{m}}$ when expanding the state $\hat{\rho}$ in these operators. Although $\boldsymbol{l},\boldsymbol{m}$ are elements of $\mathbb{Z}_{2d}$ in general, the operators $\hat{O}_{\boldsymbol{l},\boldsymbol{m}}$, and correspondingly $x_{\hat{\rho}}(\boldsymbol{l},\boldsymbol{m})$, can only gain a phase factor by a translation $l_i \to l_i + d$ and $m_i \to m_i + d$ for any $i = 1,\ldots,n$.

To show all the results in this chapter, we use the properties of the operators $\hat{O}_{l,m}$. So we want to discuss them here further. The operator $\hat{O}_{l,m}$ is a Hermitian operator $\hat{O}_{l,m} = \hat{O}_{l,m}^\dagger$ and a unitary operator $\hat{O}_{l,m}\hat{O}_{l,m}^\dagger = \mathbb{1}$ and thus

$$\hat{O}_{l,m}\hat{O}_{l,m} = \mathbb{1}, \tag{5.8}$$

implying that the spectrum is ± 1.

These operators are orthogonal in the sense of the Hilbert-Schmidt inner product

$$\operatorname{Tr}\left(\hat{O}_{l,m}\hat{O}_{l'm'}\right) = \delta_{mm'}\delta_{ll'}d. \tag{5.9}$$

Furthermore, the action of Clifford unitaries on the operators $O_{\boldsymbol{l},\boldsymbol{m}}$ is equivalent to a symplectic linear transformation on the coordinates $(\boldsymbol{l},\boldsymbol{m})$ and constant shifts.

For $d = 2$, the operators $\hat{O}_{l,m}$ are precisely the standard Pauli operators. Therefore, $\hat{O}_{l,m}$ can be seen as a Hermitian generalization of the Pauli operators to arbitrary dimensions.

The operators $\{\hat{O}_{\boldsymbol{l},\boldsymbol{m}}\}_{l,m\in\mathbb{Z}_d^n}$ form an operator basis of a n-qudit system. The proof of all of these properties can be found in Paper D.

The coefficients $c_{\rho_{\mathrm{GKP}}}(\boldsymbol{l},\boldsymbol{m})$ are unsurprisingly periodic, meaning that we can reduce the GKP Wigner function to one unit cell that is repeated in phase space. Interestingly, the atomic form separates the intrinsic CV part in the form of the Dirac distributions from the DV part that is entirely encoded in $c_{\rho_{\mathrm{GKP}}}(\boldsymbol{l},\boldsymbol{m})$ through the equivalence with $x_{\hat{\rho}}(\boldsymbol{l},\boldsymbol{m})$.

5.2 Magic measure for qubits

In Paper B we investigate this connection between CV and DV for qubits. By computing the Wigner logarithmic negativity of a GKP state encoding a pure qubit state $|\psi\rangle = \sum_{\boldsymbol{i}\in\mathbb{Z}_2^n} c_{\boldsymbol{i}} |\boldsymbol{i}\rangle$ stemming from the Wigner function Eq. 5.3 for the case of qubits and restricting the integration domain to one unit cell, we can define a GKP inspired magic measure. Even though the GKP state encoding a pure state has infinite negativity, by restricting to one unit cell $\mathcal{C}$, this becomes finite. Thus, we can define a magic measure by computing the Wigner logarithmic negativity of a GKP state and renormalizing it by the intrinsic Wigner logarithmic negativity of a pure stabilizer state in one cell. The details can be found in Paper B. The magic measure is finally obtained as

$$\begin{aligned}\mathcal{G}(|\psi\rangle) &\equiv \log_2\left[\left(\frac{\sqrt{\pi}}{2}\right)^n \int_{\mathcal{C}} \mathrm{d}\boldsymbol{q}\mathrm{d}\boldsymbol{p}\, |W_{|\psi\rangle\langle\psi|_{\mathrm{GKP}}}(\boldsymbol{q},\boldsymbol{p})|\right] \\ &= \log_2\left(\sum_{\boldsymbol{i},\boldsymbol{j}\in\mathbb{Z}_2^n}\left|\sum_{\boldsymbol{k}\in\mathbb{Z}_2^n}\frac{(-1)^{\boldsymbol{i}\cdot\boldsymbol{k}}}{2^n} c_{\boldsymbol{k}}^* c_{\boldsymbol{k}+\boldsymbol{j}}\right|\right) \qquad (5.10) \\ &= \log_2\left(\frac{1}{2^n}\sum_{\hat{P}\in\mathcal{P}_n^*}\left|\mathrm{Tr}\left[|\psi\rangle\langle\psi|\,\hat{P}\right]\right|\right). \qquad (5.11)\end{aligned}$$

$\mathcal{P}_n^*$ is the projective Pauli group, only including $+1$ phases. Surprisingly, this quantity was already studied in the name of *st-norm* and was known to be a magic witness and a lower bound for the robustness of magic [44]. However, as we will now detail, in Paper B we prove that it satisfies the relevant properties as a magic measure. Furthermore, the st-norm is connected to the $\alpha-$stabilizer Rényi entropy for $\alpha = \frac{1}{2}$ [61]. Even though the analysis started with GKP states, a continuous-variable object, and the continuous Wigner negativity, in the end, we obtain a magic measure that is useful in the resource theory of magic of qubits.

Using the properties of the Wigner logarithmic negativity enables us to demonstrate the following properties (see Chap. 3 for definitions):

1. Invariance under Clifford unitaries $\hat{U}_C$: $\mathcal{G}(\hat{U}_C|\psi\rangle) = \mathcal{G}(|\psi\rangle)$
2. Additivity: $\mathcal{G}(|\psi\rangle_A \otimes |\phi\rangle_B) = \mathcal{G}(|\psi\rangle) + \mathcal{G}(|\phi\rangle)$
3. Faithfulness: $\mathcal{G}(|\psi_S\rangle) = 0$ iff $|\psi_S\rangle$ is a stabilizer state
4. Invariance under composition with stabilizer states: $\mathcal{G}(|\psi\rangle \otimes |\phi_S\rangle) = \mathcal{G}(|\psi\rangle)$

5. Non-increasing under measurement in the computational basis: $\mathcal{G}(|\psi\rangle\langle\psi|) \geq \mathcal{G}\left(\sum_\lambda p_\lambda |\phi_\lambda\rangle\langle\phi_\lambda|\right)$ with $|\phi_\lambda\rangle\langle\phi_\lambda|)$ being the post-measurement state of outcome λ.

The significant advantage of the st-norm is its simple computation for quantum states. Aided by the fact that it is additive, it is possible to investigate larger qubit systems. Since evaluating the $st-$norm is equivalent to computing Pauli expectation values, analytical derivations can easily be made. Even though the st-norm has enormous advantages, it also has drawbacks. First, the measure is only valid for pure states and not mixed states, which heavily restricts the use cases. One could consider convex roof constructions [108]. However, this would imply losing the advantage of being computable, since it involves optimizing over all possible ensembles that represent the mixed state. An even more significant drawback is the limited set of free operations. Computational basis measurements as defined in Chap. 3 and tracing out sub-systems are not included, restricting the use cases even further.

5.3 Magic measure for qudits

5.3.1 Wigner function

In Paper D we study the generalization to general qudits and give a simulation algorithm which runtime scales with the magic quantifier we defined. We show that the p-norm of $x_{\hat{\rho}}(\boldsymbol{l}, \boldsymbol{m})$ appearing in Eq. (5.3) is directly connected to renormalized generalized Wigner negativity of the GKP encoded state.

In the following, we also consider the l_p-norm of a function $f : \mathbb{Z}_d^{2n} \to \mathbb{C}$ defined by

$$\|f\|_p = \left(\sum_{\boldsymbol{u} \in \mathbb{Z}_d^{2n}} |f(\boldsymbol{u})|^p \right)^{1/p} \tag{5.12}$$

Similarly to the case of discrete variables, we also consider a l_p-norm for a function $f : \mathbb{R}^{2n} \to \mathbb{C}$ defined by

$$\|f\|_p = \left(\int_{\mathbb{R}^{2n}} \mathrm{d}\boldsymbol{r} |f(\boldsymbol{r})|^p \right)^{1/p}. \tag{5.13}$$

Note that for $p = 1$, we recover the negativities we discussed before. The exact result is as follows:

Theorem 3. *For an n-qudit state $\hat{\rho}$ on a d^n-dimensional space and for an arbitrary real number $p > 0$, it holds that*

$$d^{n(1-1/p)}\|x_{\hat{\rho}}\|_p = \frac{\|W^{\mathrm{CV}}_{\hat{\rho}_{\mathrm{GKP}}}\|_{p,\mathrm{cell}}}{\|W^{\mathrm{CV}}_{\mathrm{STAB}_n,\mathrm{GKP}}\|_{p,\mathrm{cell}}}, \tag{5.14}$$

where

$$\|W^{\mathrm{CV}}_{\mathrm{STAB}_n,\mathrm{GKP}}\|_{p,\mathrm{cell}} \coloneqq \|W^{\mathrm{CV}}_{\hat{\phi}_{\mathrm{GKP}}}\|_{p,\mathrm{cell}} \tag{5.15}$$

$$= (4d)^{n/p}/(8\pi d)^{n/2} \tag{5.16}$$

is a quantity that takes the same value for every n-qudit pure stabilizer state $\hat{\phi}$. When d is odd, an even stronger result holds

$$d^{n(1-1/p)}\left\|x_{\hat{\rho}}\right\|_p = d^{n(1-1/p)}\|W^{\mathrm{DV}}_{\hat{\rho}}\|_p = \frac{\|W^{\mathrm{CV}}_{\hat{\rho}_{\mathrm{GKP}}}\|_{p,\mathrm{cell}}}{\|W^{\mathrm{CV}}_{\mathrm{STAB}_n,\mathrm{GKP}}\|_{p,\mathrm{cell}}}. \tag{5.17}$$

The interpretation of Eq. (5.17) is as follows: Surprisingly, for $p = 1$ and odd dimensions, the renormalized negativity of continuous Wigner of a GKP state restricted to one unit is equivalent to the discrete Wigner negativity of the corresponding quantum state. By setting $p = 1$ and $d = 2$ in Eq. (5.14), we recover exactly the results from the previous section, i.e., the result we obtained for qubits. Furthermore, we can use (5.14) to generalize the result of the previous section to all dimensions. We, therefore, set $p = 1$ and obtain magic quantifiers for all dimensions. We notice that the qudit dimension heavily determines the properties of the magic quantifiers we defined here. For odd dimensions, the quantifier is equivalent to the discrete Wigner negativity which gives us the properties of the magic measure directly, namely monotonicity under stabilizer protocols and multiplicativity. More generally, for even dimensions, we have to restrict it to pure states, as was the case for qubits. In the more general case of arbitrary qudit dimensions, the properties are similar to the one of the $st-$norm shown above:

1. Invariance under Clifford unitaries U_C:
   $\left\|x_{U_C\hat{\rho}U_C^\dagger}\right\|_1 = \left\|x_{\hat{\rho}}\right\|_1$
2. Multiplicativity: $\left\|x_{\hat{\rho}\otimes\hat{\sigma}}\right\|_1 = \left\|x_{\hat{\rho}}\right\|_1\|x_{\hat{\sigma}}\|_1$
3. Stabilizer states achieve the minimum value:
   $\|x_{\hat{\phi}}\|_1 = 1$ for every pure stabilizer state $\hat{\phi}$, and $\|x_{\hat{\psi}}\|_1 \geq 1$ for every pure state ψ.

For even dimensions, the magic quantifiers we defined here have the same drawbacks as we have seen for the qubit case. Even though they are easy to compute and allow for analytical evaluation, the restricted set of free operations and the limitation to free states, limit the use cases.

5.3.2 Characteristic function

We can do a similar analysis for the characteristic function of GKP states. The characteristic function of a qudit encoded in GKP can then be written as

$$\begin{aligned}&\chi^{\mathrm{CV}}_{\hat{\rho}_{\mathrm{GKP}}}(\boldsymbol{r})\\&=\sqrt{\frac{2\pi}{d}}\sum_{\boldsymbol{l},\boldsymbol{m}=-\infty}^{\infty}\gamma_{\rho_{\mathrm{GKP}}}(\boldsymbol{l},\boldsymbol{m})\delta\left(\boldsymbol{p}-\boldsymbol{m}\sqrt{\frac{2\pi}{d}}\right)\delta\left(\boldsymbol{q}-\boldsymbol{l}\sqrt{\frac{2\pi}{d}}\right).\end{aligned}\tag{5.18}$$

The coefficients $\gamma_{\rho_{\mathrm{GKP}}}(l,m)$ are directly connected with the characteristic function of the encoded state ρ:

Theorem 4. *Let ρ be an n-qudit state on a d^n-dimensional space. For $\boldsymbol{l},\boldsymbol{m}\in\mathbb{Z}^n_{2d}$, it holds that*

$$\gamma_{\hat{\rho}_{\mathrm{GKP}}}(\boldsymbol{l},\boldsymbol{m})=d^n\omega_d^{-\boldsymbol{l}\cdot\boldsymbol{m}/2}\omega_D^{-\boldsymbol{l}\cdot\boldsymbol{m}/2}\chi^{\mathrm{DV}}_{\hat{\rho}}(\boldsymbol{l},\boldsymbol{m})^*\tag{5.19}$$

In particular,

$$d^{n(1-1/p)}\|\chi^{\mathrm{DV}}_{\hat{\rho}}\|_p=\frac{\|\chi^{\mathrm{CV}}_{\hat{\rho}_{\mathrm{GKP}}}\|_{p,\mathrm{cell}}}{\|\chi^{\mathrm{CV}}_{\mathrm{STAB,GKP}}\|_{p,\mathrm{cell}}}\tag{5.20}$$

where

$$\|\chi^{\mathrm{CV}}_{\mathrm{STAB,GKP}}\|_{p,\mathrm{cell}}\coloneqq\|\chi^{\mathrm{CV}}_{\hat{\phi}_{\mathrm{GKP}}}\|_{p,\mathrm{cell}}\tag{5.21}$$

$$=\left(\frac{2\pi}{d}\right)^{n/2}(4d)^{n/p}\tag{5.22}$$

is a quantity that takes the same value for every pure stabilizer state $\hat{\phi}$.

In particular, this result allows us to connect the $p-$ norm of the continuous characteristic function of a GKP state with a generalization of the $\alpha-$stabilizer Rényi entropy. The natural extension of the $\alpha-$stabilizer Rényi entropy [61] to n-qudit state is

$$\begin{aligned}&M_\alpha(\hat{\rho})\\&=(1-\alpha)^{-1}\log\left(d^{-n\alpha}\sum_{\hat{P}\in\mathcal{P}_n^*}\left|\mathrm{Tr}\left(\hat{\rho}\hat{P}\right)\right|^{2\alpha}\right)-n\log d\\&=\alpha(1-\alpha)^{-1}\log\left\|\Xi(\hat{\rho})\right\|_\alpha-n\log d\end{aligned}\tag{5.23}$$

where $\mathcal{P}_n^*$ is the projective generalized Pauli (Heisenberg-Weyl) group which only contains $+1$ phase, $\Xi_{\hat{P}}(\hat{\rho})=\frac{1}{d^n}\mathrm{Tr}\left(\hat{\rho}\hat{P}\right)^2$ and forms a probability distribution when ρ is pure.

Thus, we see immediately by comparing Eq. (5.23) and the l_p norm of the discrete characteristic function $\left\|\chi_{\hat{\rho}}^{\mathrm{DV}}\right\|_p$ that we can write all α-stabilizer Rényi entropies with the $l_{2\alpha}$-norm of the continuous-variable characteristic function for the qudit state that the GKP state encodes. Specifically, we have

$$M_\alpha(\hat{\rho}) = \frac{2\alpha}{1-\alpha}\log\|\chi_{\hat{\rho}}^{\mathrm{DV}}\|_{2\alpha} - n\log d \tag{5.24}$$

$$= \frac{2\alpha}{1-\alpha}\log\frac{\|\chi_{\hat{\rho}_{\mathrm{GKP}}}^{\mathrm{CV}}\|_{2\alpha,\mathrm{cell}}}{\|\chi_{\mathrm{STAB,GKP}}^{\mathrm{CV}}\|_{2\alpha,\mathrm{cell}}} - \frac{\alpha\, n\log d}{1-\alpha}. \tag{5.25}$$

5.3.3 Applications

Our unified treatment of magic quantification in all dimensions allows us to put forward classical simulation algorithms whose runtime scale with resource content of the $p = 1$ norm of the discrete characteristic function $x_{\hat{\rho}}$ and $\chi_{\hat{\rho}}^{\mathrm{DV}}$ respectively. The aim is a strong simulation algorithm that computes the Born probability $P(\hat{\Pi}|\hat{U}\hat{\rho}\hat{U}^\dagger)$ of obtaining a measurement result corresponding to the projector $\hat{\Pi}$ of an input state $\hat{\rho}$ after we applied some unitaries $\hat{U}$. A strong simulation algorithm computes the output probability for a given measurement outcome. A detailed presentation can be found in Paper D. Similar to defining the quantity $x_{\hat{\rho}}(\lambda)$, where we used the notation $\boldsymbol{\lambda} = \boldsymbol{l}, \boldsymbol{m}$, we can define similar quantities for measurements and effects of unitary operators

$$x_{\hat{\rho}}(\boldsymbol{\lambda}) = \mathrm{Tr}\left(\hat{\rho}\frac{\hat{O}_{\boldsymbol{\lambda}}}{d^n}\right) \tag{5.26}$$

$$x_{\hat{U}}(\boldsymbol{\lambda}', \boldsymbol{\lambda}) = \mathrm{Tr}\left(\frac{\hat{O}_{\boldsymbol{\lambda}'}}{d^n}\hat{U}\hat{O}_{\boldsymbol{\lambda}}\hat{U}^\dagger\right) \tag{5.27}$$

$$x_{\hat{\Pi}}(\boldsymbol{\lambda}) = \mathrm{Tr}\left(\hat{\Pi}\hat{O}_{\boldsymbol{\lambda}}\right). \tag{5.28}$$

This can be seen when we expand the state and the effect of unitary operators and measurements in the basis $\hat{O}_{\boldsymbol{\lambda}}$. We can do the same using the characteristic function and expanding everything in Heisenberg-Weyl operators $\hat{P}(\boldsymbol{\lambda})$

$$\chi_{\hat{\rho}}^{\mathrm{DV}}(\boldsymbol{\lambda}) = \mathrm{Tr}\left(\hat{\rho}\frac{\hat{P}^\dagger(\boldsymbol{\lambda})}{d^n}\right) \tag{5.29}$$

$$\chi_{\hat{U}}^{\mathrm{DV}}(\boldsymbol{\lambda}', \boldsymbol{\lambda}) = \mathrm{Tr}\left(\frac{\hat{P}^\dagger(\boldsymbol{\lambda}')}{d^n}\hat{U}\hat{P}(\boldsymbol{\lambda})\hat{U}^\dagger\right) \tag{5.30}$$

$$\chi_{\hat{\Pi}}^{\mathrm{DV}}(\boldsymbol{\lambda}') = \mathrm{Tr}\left(\hat{\Pi}\hat{P}(\boldsymbol{\lambda})\right). \tag{5.31}$$

We describe the algorithm in terms of the quantities x, but it works equivalently for χ. From the quantities $x_{\hat{\rho}}(\boldsymbol{\lambda})$ we can define the probability distributions

$$P(\boldsymbol{\lambda}|\rho) = \frac{\left|x_{\hat{\rho}}(\boldsymbol{\lambda})\right|}{\left\|x_{\hat{\rho}}\right\|_1} \tag{5.32}$$

$$P(\boldsymbol{\lambda}'|\hat{U},\boldsymbol{\lambda}) = \frac{\left|x_{\hat{U}}(\boldsymbol{\lambda}',\boldsymbol{\lambda})\right|}{\left\|x_{\hat{U}}(\boldsymbol{\lambda})\right\|_1} \tag{5.33}$$

$$\left\|x_{\hat{U}}(\boldsymbol{\lambda})\right\|_1 = \sum_{\boldsymbol{\lambda}'} \left|x_{\hat{U}}(\boldsymbol{\lambda}',\boldsymbol{\lambda})\right| \tag{5.34}$$

$$\left\|x_{\hat{\rho}}\right\|_1 = \sum_{\boldsymbol{\lambda}} \left|x_{\hat{\rho}}(\boldsymbol{\lambda})\right|. \tag{5.35}$$

Thus, we can rewrite the Born rule probability as

$$P(\hat{\Pi}|\hat{U}\hat{\rho}\hat{U}^\dagger) = \mathrm{Tr}\left[\hat{P}\hat{U}\hat{\rho}\hat{U}^\dagger\right] \tag{5.36}$$

$$= \sum_{\boldsymbol{\lambda},\boldsymbol{\lambda}'} x_{\hat{\Pi}}(\boldsymbol{\lambda}')x_{\hat{U}}(\boldsymbol{\lambda}',\boldsymbol{\lambda})x_{\hat{\rho}}(\boldsymbol{\lambda}) \tag{5.37}$$

$$= \sum_{\boldsymbol{\lambda},\boldsymbol{\lambda}'} M_{\boldsymbol{\lambda},\boldsymbol{\lambda}'} P(\boldsymbol{\lambda}'|\hat{U},\boldsymbol{\lambda})P(\boldsymbol{\lambda}|\rho) \tag{5.38}$$

with $M_{\boldsymbol{\lambda},\boldsymbol{\lambda}'} = \mathrm{sign}\big(x_{\hat{\Pi}}(\boldsymbol{\lambda}')x_{\hat{U}}(\boldsymbol{\lambda}',\boldsymbol{\lambda})\big)x_{\hat{\Pi}}(\boldsymbol{\lambda}')\left\|x_{\hat{U}}(\boldsymbol{\lambda})\right\|_1\left\|x_{\hat{\rho}}\right\|_1$. We used that the operators $\hat{O}_{\boldsymbol{\lambda}}$ form a orthogonal basis and expanded $\hat{\Pi}$, $\hat{\rho}$ and the effect of $\hat{U}$ in that basis.

The simulation strategy is then to sample $\boldsymbol{\lambda}$ from $P(\boldsymbol{\lambda}|\rho)$ and then consider a possible transition to $\boldsymbol{\lambda}'$ from $P(\boldsymbol{\lambda}'|\hat{U},\boldsymbol{\lambda})$. This can easily be generalized to a sequence of unitaries of length T as well. We then define a random variable as

$$M_{\vec{\boldsymbol{\lambda}}} = x_{\hat{\Pi}}(\boldsymbol{\lambda}_T)\mathrm{sign}(x_{\hat{\rho}}(\boldsymbol{\lambda}_0))\left\|x_{\hat{\rho}}\right\|_1 \tag{5.39}$$

$$\times \prod_{t=1}^{T} \mathrm{sign}(x_{\hat{U}_t}(\boldsymbol{\lambda}_t,\boldsymbol{\lambda}_{t-1}))\left\|x_{\hat{U}_t}(\boldsymbol{\lambda}_{t-1})\right\|_1. \tag{5.40}$$

The expectation value of this random variable is

$$\mathbb{E}(M_{\vec{\boldsymbol{\lambda}}}) = \sum_{\vec{\boldsymbol{\lambda}}} P(\boldsymbol{\lambda}_0|\rho)\prod_{t=1}^{T} P(\boldsymbol{\lambda}_t|\hat{U}_t,\boldsymbol{\lambda}_{t-1})M_{\vec{\boldsymbol{\lambda}}} \tag{5.41}$$

$$= \sum_{\vec{\boldsymbol{\lambda}}} x_{\hat{\Pi}}(\boldsymbol{\lambda}_T)\prod_{t=1}^{T} x_{\hat{U}_t}(\boldsymbol{\lambda}_t,\boldsymbol{\lambda}_{t-1})x_{\hat{\rho}}(\boldsymbol{\lambda}_0) \tag{5.42}$$

which is exactly the Born probability we want to estimate. The random variable output from our sampling algorithm is an unbiased estimator for the Born probability. The

sampling cost/the number of samples required to estimate the Born probability up to error ϵ with failure probability p_f is

$$K \geq 2\mathcal{M}_{\rightarrow}^2 \frac{1}{\epsilon^2} \ln\left(\frac{2}{p_f}\right), \tag{5.43}$$

where $\mathcal{M}_{\rightarrow}$ is the negativity of the entire circuit and is given as

$$\mathcal{M}_{\rightarrow} = \left\|x_{\hat{\rho}}\right\|_1 \prod_{t=1} \max_{\boldsymbol{\lambda}_t} \left\|x_{\hat{U}_t}(\boldsymbol{\lambda}_t)\right\|_1 \max_{\boldsymbol{\lambda}_T} \left|x_{\hat{\Pi}}(\boldsymbol{\lambda}_T)\right|. \tag{5.44}$$

For $\hat{U}$ being a Clifford unitary, $\left\|x_{\hat{U}_t}(\boldsymbol{\lambda}_t)\right\|_1$ is $= 1$, and the simulation cost is the resource content of the initial state $\left\|x_{\hat{\rho}}\right\|_1$, while the cost of measurements needs a bit more discussion. In the case of the discrete characteristic function and even dimension for $x_{\hat{\rho}}$, the simulator has some interesting behavior. If not all qudits are measured, measurements affect the simulation cost. This is not surprising since measurements cannot be included in the set of free operations in this case.

Let us assume that we would like to measure k-qudits of our n-qudit system in a computational basis state $|\boldsymbol{i}\rangle = |i_1\rangle \otimes ... |i_n\rangle$. The measurement effect then is given as $\hat{\Pi} = \mathbb{1}_{n-k} \otimes |\boldsymbol{i}\rangle\langle\boldsymbol{i}|$. Without loss of generality, we assume a specific measurement outcome, i.e., measurement of the state $|\mathbf{1}\rangle\langle\mathbf{1}|$, with all measured qudits in the 1 state. The expansion of one qudit state$|1\rangle\langle 1|$ in the operators $\hat{O}_{l,m}$ is $|1\rangle\langle 1| = \frac{1}{d}\sum_{i=1}^{d-1} \hat{O}_{2,i}$. The cost inferred from the measurement is then

$$\max_{\boldsymbol{\lambda}_T} \left|x_{\hat{\Pi}}(\boldsymbol{\lambda}_T)\right| = \max_{\boldsymbol{l},\boldsymbol{m}} \left|\mathrm{Tr}\left[\hat{O}_{\boldsymbol{l},\boldsymbol{m}} \mathbb{1}_{n-k} \otimes |\mathbf{1}\rangle\langle\mathbf{1}|\right]\right| \tag{5.45}$$

$$= \max_{\boldsymbol{l_{n-k}},\boldsymbol{m_{n-k}}} \left|\mathrm{Tr}\left[\hat{O}_{\boldsymbol{l_{n-k}},\boldsymbol{m_{n-k}}}\right]\right| \max_{\boldsymbol{l_k},\boldsymbol{m_k}} \left|\mathrm{Tr}\left[\hat{O}_{\boldsymbol{l_k},\boldsymbol{m_k}} |\mathbf{1}\rangle\langle\mathbf{1}|\right]\right| \tag{5.46}$$

The maximum trace $\left|\mathrm{Tr}\left[\hat{O}_{\boldsymbol{l_k},\boldsymbol{m_k}} |\mathbf{1}\rangle\langle\mathbf{1}|\right]\right|$ is 1 for both even and odd dimensions. However, there is a big difference between even and odd dimensions for the first term. For odd dimensions, the trace of $O_{\boldsymbol{l},\boldsymbol{m}}$ is ± 1, so unmeasured qudits do not add to the simulation cost in any way. This is not the case for even dimensions. In even dimensions, the trace of a single qudit operator $\hat{O}_{l,m}$ is either 0 or 2. Therefore, the maximum of the first term $\left|\mathrm{Tr}\left[\hat{O}_{\boldsymbol{l_{n-k}},\boldsymbol{m_{n-k}}}\right]\right|$ is 2^{n-k}, and thus the number of unmeasured qudits increase the number of samples required exponentially. So we see that for odd dimensional systems, computational basis measurements do not increase the simulation cost and for Clifford operations the entire cost is given by the input state. For even dimensional systems, the measurements can increase the sampling cost significantly.

We can also use our findings to prove results for continuous variables. Using the connection between the resource theory of non-Gaussianty and Wigner negativity, we prove that genuine non-Gaussian resources are needed to implement a non-stabilizer operation on the code subspace.

Theorem 5. *Let Λ be a quantum channel with n-qubit input and n-qubit output. If there exists a pure stabilizer state $\hat{\phi}$ and a pure non-stabilizer state $\hat{\psi}$ such that $\Lambda\left(\hat{\phi}\right) = \hat{\psi}$, then Λ cannot be implemented in a GKP code space by a Gaussian protocol. Also, for a quantum channel Λ with n-qudit input and n-qudit output systems with odd local dimensions, the condition can be relaxed to the existence of a (potentially mixed) stabilizer state $\hat{\sigma}$ and a state $\hat{\rho}$ with $\|W_{\hat{\rho}}^{\mathrm{DV}}\|_1 > 1$ such that $\Lambda(\hat{\sigma}) = \hat{\rho}$.*

Chapter 6

Conclusion

Tremendous progress in controlling quantum systems opened up many new applications. This has led to rapid advancement in quantum technologies, with quantum computing being one of the most prominent applications. This thesis focused on studying resources for quantum computing in discrete and continuous-variable systems. We investigated the generation and inter-conversion of resource states for continuous variable systems. We studied the quantification of magic in qudit systems by connecting the resource theory of genuine non-Gaussianity with the resource theory of magic.

In Chap. 4, we studied the inter-conversion and generation of non-Gaussian states that are of interest for quantum computing. We considered Gaussian protocols, which can be easily implemented in quantum optical setups. We discussed converting the trisqueezed state to the cubic phase state studied in Paper A. We provided a deterministic and a probabilistic protocol that obtains a high-fidelity conversion. The probabilistic protocol even reproduced the very intricate features of the cubic phase state. Then we discussed a result of Paper C the conversion from photon subtracted states to cat states. By employing a deterministic Gaussian protocol, one can significantly improve the conversion. Our extensive numerical study of 1-to-1 deterministic Gaussian conversions showed that the results are very limited in their usefulness. The next step would be to start studying protocols that reduce the number of modes –cascading Gaussian protocols– or include post-selection. The inclusion of post-selection would especially open new avenues for interesting Gaussian conversions.

At last, in Chap. 5 we investigated the resource theory of magic and introduced new continuous-variable inspired magic quantifiers. In Paper B we considered qubit systems. By computing the Wigner negativity of a GKP state encoding a pure quantum state and re-normalizing this quantity, we could define a magic measure for qubits. Interestingly, the obtained quantity was known in the literature as the st-norm. Then, we generalized this approach to arbitrary qudit dimensions, as can be read in Paper D. We found a direct connection between the continuous Wigner function of a GKP state

and the discrete Wigner function of the encoded state for odd-dimensional systems. The magic quantifier thus reduces to the discrete Wigner negativity for odd-dimensional systems but is defined for all dimensions. We furthermore provide a classical simulation algorithm that scales with the non-stabilizerness of the computation.

While we succeeded in rediscovering the discrete Wigner negativity, we found magic quantifiers for even dimensions with very restricted applicability. Although they quantify the simulation cost, they do not allow to tackle mixed states, neither they display monotonicity under measurements, which restricts the use cases. Finding a computable magic monotone that is a monotone for stabilizer protocols and quantifies the classical simulation cost for qubits or all dimensions is still desirable.

Another interesting point stemming from our work is that, as we have seen, even and odd-dimensional systems have vastly different properties. It is interesting to ask: Does it matter if the basic building blocks of the quantum computer are odd or even dimensional? Can one show a practical advantage of using, for example, odd-dimensional systems instead of qubits beyond a trivial reduction of required qudits?

Ultimately, resource theories were introduced to study the difference between a restricted and classical set of states and the rest, which is the whole set of states, operations, and measurements associated with a system. Thus, it is natural to ask what phenomenon or resource is relevant for genuine quantum computing or quantum advantage. What properties of quantum mechanics would allow us to go beyond classical computers, and how can we use that fact to improve algorithms?

Bibliography

[1] S. Krinner, N. Lacroix, A. Remm, A. Di Paolo, E. Genois, C. Leroux, C. Hellings, S. Lazar, F. Swiadek, J. Herrmann, G. J. Norris, C. K. Andersen, M. Müller, A. Blais, C. Eichler, and A. Wallraff, "Realizing repeated quantum error correction in a distance-three surface code", Nature **605**, 669-674 (2022).

[2] V. Sivak, A. Eickbusch, B. Royer, S. Singh, I. Tsioutsios, S. Ganjam, A. Miano, B. Brock, A. Ding, L. Frunzio, *et al.*, "Real-time quantum error correction beyond break-even", Nature **616**, 50–55 (2023).

[3] D. Bluvstein, S. J. Evered, A. A. Geim, S. H. Li, H. Zhou, T. Manovitz, S. Ebadi, M. Cain, M. Kalinowski, D. Hangleiter, J. P. Bonilla Ataides, N. Maskara, I. Cong, X. Gao, P. Sales Rodriguez, T. Karolyshyn, G. Semeghini, M. J. Gullans, M. Greiner, V. Vuletić, and M. D. Lukin, "Logical quantum processor based on reconfigurable atom arrays", Nature **626**, 58-65 (2024).

[4] T. M. Graham, Y. Song, J. Scott, C. Poole, L. Phuttitarn, K. Jooya, P. Eichler, X. Jiang, A. Marra, B. Grinkemeyer, M. Kwon, M. Ebert, J. Cherek, M. T. Lichtman, M. Gillette, J. Gilbert, D. Bowman, T. Ballance, C. Campbell, E. D. Dahl, O. Crawford, N. S. Blunt, B. Rogers, T. Noel, and M. Saffman, "Multi-qubit entanglement and algorithms on a neutral-atom quantum computer", Nature **604**, 457-462 (2022).

[5] M. Gulka, D. Wirtitsch, V. Ivády, J. Vodnik, J. Hruby, G. Magchiels, E. Bourgeois, A. Gali, M. Trupke, and M. Nesladek, "Room-temperature control and electrical readout of individual nitrogen-vacancy nuclear spins", Nature Communications **12**, 4421 (2021).

[6] A. G. Fowler, M. Mariantoni, J. M. Martinis, and A. N. Cleland, "Surface codes: Towards practical large-scale quantum computation", Phys. Rev. A **86**, 032324 (2012).

[7] B. Eastin and E. Knill, "Restrictions on transversal encoded quantum gate sets", Phys. Rev. Lett. **102**, 110502 (2009).

[8] D. Gottesman, "Theory of fault-tolerant quantum computation", Phys. Rev. A **57**, 127–137 (1998).

[9] D. Gottesman, *The Heisenberg representation of quantum computers*, Group22: Proceedings of the XXII International Colloquium on Group Theoretical Methods in Physics (Cambridge, MA, International Press, 1999) pp. 32–43.

[10] D. Gottesman and I. L. Chuang, "Demonstrating the viability of universal quantum computation using teleportation and single-qubit operations", Nature **402**, 390–393 (1999).

[11] S. Bravyi and A. Kitaev, "Universal quantum computation with ideal clifford gates and noisy ancillas", Phys. Rev. A **71**, 022316 (2005).

[12] C. Gidney and M. Ekerå, "How to factor 2048 bit RSA integers in 8 hours using 20 million noisy qubits", Quantum **5**, 433 (2021).

[13] O. Pfister, "Continuous-variable quantum computing in the quantum optical frequency comb", Journal of Physics B: Atomic, Molecular and Optical Physics **53**, 012001 (2020).

[14] A. Blais, A. L. Grimsmo, S. M. Girvin, and A. Wallraff, in *Mesoscopic Physics meets Quantum Engineering* (WORLD SCIENTIFIC, 2019) pp. 135–153.

[15] A. L. Grimsmo and A. Blais, "Squeezing and quantum state engineering with Josephson travelling wave amplifiers", npj Quantum Information **3**, 20 (2017).

[16] T. Hillmann, F. Quijandría, G. Johansson, A. Ferraro, S. Gasparinetti, and G. Ferrini, "Universal Gate Set for Continuous-Variable Quantum Computation with Microwave Circuits", Physical Review Letters **125**, 160501 (2020).

[17] M. Schmidt, M. Ludwig, and F. Marquardt, "Optomechanical circuits for nanomechanical continuous variable quantum state processing", New Journal of Physics **14**, 125005 (2012).

[18] O. Houhou, H. Aissaoui, and A. Ferraro, "Generation of cluster states in optomechanical quantum systems", Physical Review A **92**, 063843 (2015).

[19] W. H. P. Nielsen, Y. Tsaturyan, C. B. Møller, E. S. Polzik, and A. Schliesser, "Multimode optomechanical system in the quantum regime", Proceedings of the National Academy of Sciences **114**, 62–66 (2017).

[20] J. Stasińska, C. Rodó, S. Paganelli, G. Birkl, and A. Sanpera, "Manipulating mesoscopic multipartite entanglement with atom-light interfaces", Physical Review A **80**, 062304 (2009).

[21] D. F. Milne and N. V. Korolkova, "Composite-cluster states and alternative architectures for one-way quantum computation", Physical Review A **85**, 032310 (2012).

[22] Y. Ikeda and N. Yamamoto, "Deterministic generation of Gaussian pure states in a quasilocal dissipative system", Physical Review A **87**, 033802 (2013).

[23] K. R. Motes, B. Q. Baragiola, A. Gilchrist, and N. C. Menicucci, "Encoding qubits into oscillators with atomic ensembles and squeezed light", Physical Review A **95**, 053819 (2017).

[24] S. Lloyd and S. L. Braunstein, in *Quantum Information with Continuous Variables* (Springer, 1999) pp. 9–17.

[25] D. Gottesman, A. Kitaev, and J. Preskill, "Encoding a qubit in an oscillator", Physical Review A **64**, 012310 (2001).

[26] A. Mari and J. Eisert, "Positive wigner functions render classical simulation of quantum computation efficient", Phys. Rev. Lett. **109**, 230503 (2012).

[27] J. Niset, J. Fiurášek, and N. J. Cerf, "No-go theorem for gaussian quantum error correction", Phys. Rev. Lett. **102**, 120501 (2009).

[28] J. Yoshikawa, S. Yokoyama, T. Kaji, C. Sornphiphatphong, Y. Shiozawa, K. Makino, and A. Furusawa, "Invited article: Generation of one-million-mode continuous-variable cluster state by unlimited time-domain multiplexing", APL Photonics **1**, 060801 (2016).

[29] N. Ofek, A. Petrenko, R. Heeres, P. Reinhold, Z. Leghtas, B. Vlastakis, Y. Liu, L. Frunzio, S. M. Girvin, L. Jiang, M. Mirrahimi, M. H. Devoret, and R. J. Schoelkopf, "Extending the lifetime of a quantum bit with error correction in superconducting circuits", Nature **536**, 441–445 (2016).

[30] A. L. Grimsmo and S. Puri, "Quantum error correction with the gottesman-kitaev-preskill code", PRX Quantum **2**, 020101 (2021).

[31] B. M. Terhal, J. Conrad, and C. Vuillot, "Towards scalable bosonic quantum error correction", Quantum Science and Technology **5**, 043001 (2020).

[32] W. Cai, Y. Ma, W. Wang, C.-L. Zou, and L. Sun, "Bosonic quantum error correction codes in superconducting quantum circuits", Fundamental Research **1**, 50-67 (2021).

[33] W.-L. Ma, S. Puri, R. J. Schoelkopf, M. H. Devoret, S. Girvin, and L. Jiang, "Quantum control of bosonic modes with superconducting circuits", Science Bulletin **66**, 1789-1805 (2021).

[34] S. Konno, W. Asavanant, F. Hanamura, H. Nagayoshi, K. Fukui, A. Sakaguchi, R. Ide, F. China, M. Yabuno, S. Miki, H. Terai, K. Takase, M. Endo, P. Marek, R. Filip, P. van Loock, and A. Furusawa, "Logical states for fault-tolerant quantum computation with propagating light", Science **383**, 289-293 (2024).

[35] A. L. Grimsmo, J. Combes, and B. Q. Baragiola, "Quantum Computing with Rotation-Symmetric Bosonic Codes", Physical Review X **10**, 011058 (2020).

[36] D. Stick, W. K. Hensinger, S. Olmschenk, M. J. Madsen, K. Schwab, and C. Monroe, "Ion trap in a semiconductor chip", Nature Physics **2**, 36-39 (2006).

[37] M. Horodecki, P. Horodecki, and R. Horodecki, "General teleportation channel, singlet fraction, and quasidistillation", Phys. Rev. A **60**, 1888–1898 (1999).

[38] V. Coffman, J. Kundu, and W. K. Wootters, "Distributed entanglement", Phys. Rev. A **61**, 052306 (2000).

[39] T. J. Osborne and F. Verstraete, "General monogamy inequality for bipartite qubit entanglement", Phys. Rev. Lett. **96**, 220503 (2006).

[40] A. Streltsov, G. Adesso, and M. B. Plenio, "Colloquium: Quantum coherence as a resource", Rev. Mod. Phys. **89**, 041003 (2017).

[41] S. Bravyi and D. Gosset, "Improved classical simulation of quantum circuits dominated by clifford gates", Phys. Rev. Lett. **116**, 250501 (2016).

[42] S. Bravyi, G. Smith, and J. A. Smolin, "Trading classical and quantum computational resources", Phys. Rev. X **6**, 021043 (2016).

[43] S. Bravyi, D. Browne, P. Calpin, E. Campbell, D. Gosset, and M. Howard, "Simulation of quantum circuits by low-rank stabilizer decompositions", Quantum **3**, 181 (2019).

[44] M. Howard and E. Campbell, "Application of a resource theory for magic states to fault-tolerant quantum computing", Phys. Rev. Lett. **118**, 090501 (2017).

[45] J. R. Seddon, B. Regula, H. Pashayan, Y. Ouyang, and E. T. Campbell, "Quantifying quantum speedups: Improved classical simulation from tighter magic monotones", PRX Quantum **2**, 010345 (2021).

[46] M. G. Genoni, M. G. A. Paris, and K. Banaszek, "Measure of the non-gaussian character of a quantum state", Phys. Rev. A **76**, 042327 (2007).

[47] M. G. Genoni, M. G. A. Paris, and K. Banaszek, "Quantifying the non-gaussian character of a quantum state by quantum relative entropy", Phys. Rev. A **78**, 060303 (2008).

[48] R. Takagi and Q. Zhuang, "Convex resource theory of non-Gaussianity", Phys. Rev. A **97**, 062337 (2018).

[49] F. Albarelli, M. G. Genoni, M. G. A. Paris, and A. Ferraro, "Resource theory of quantum non-gaussianity and wigner negativity", Phys. Rev. A **98**, 052350 (2018).

[50] U. Chabaud, D. Markham, and F. Grosshans, "Stellar representation of non-gaussian quantum states", Phys. Rev. Lett. **124**, 063605 (2020).

[51] B. Regula, L. Lami, G. Ferrari, and R. Takagi, "Operational quantification of continuous-variable quantum resources", Phys. Rev. Lett. **126**, 110403 (2021).

[52] L. Lami, B. Regula, R. Takagi, and G. Ferrari, "Framework for resource quantification in infinite-dimensional general probabilistic theories", Phys. Rev. A **103**, 032424 (2021).

[53] A. Kenfack and K. Życzkowski, "Negativity of the wigner function as an indicator of non-classicality", J. Opt. B: Quantum Semiclass. Opt. **6**, 396 (2004).

[54] V. Veitch, N. Wiebe, C. Ferrie, and J. Emerson, "Efficient simulation scheme for a class of quantum optics experiments with non-negative wigner representation", New Journal of Physics **15**, 013037 (2013).

[55] D. Gross, *Finite phase space methods in quantum information*, Ph.D. thesis, Diploma Thesis, Potsdam (2005).

[56] D. Gross, "Hudson's theorem for finite-dimensional quantum systems", J. Math. Phys. **47**, 122107 (2006).

[57] V. Veitch, C. Ferrie, D. Gross, and J. Emerson, "Negative quasi-probability as a resource for quantum computation", New J. Phys. **14**, 113011 (2012).

[58] V. Veitch, S. A. H. Mousavian, D. Gottesman, and J. Emerson, "The resource theory of stabilizer quantum computation", New J. Phys. **16**, 013009 (2014).

[59] B. Regula, "Convex geometry of quantum resource quantification", J. Phys. A: Math. Theor. **51**, 045303 (2017).

[60] M. Beverland, E. Campbell, M. Howard, and V. Kliuchnikov, "Lower bounds on the non-clifford resources for quantum computations", Quantum Science and Technology **5**, 035009 (2020).

[61] L. Leone, S. F. E. Oliviero, and A. Hamma, "Stabilizer rényi entropy", Phys. Rev. Lett. **128**, 050402 (2022).

[62] T. Haug and M. Kim, "Scalable measures of magic resource for quantum computers", PRX Quantum **4**, 010301 (2023).

[63] R. Raussendorf, D. E. Browne, N. Delfosse, C. Okay, and J. Bermejo-Vega, "Contextuality and wigner-function negativity in qubit quantum computation", Phys. Rev. A **95**, 052334 (2017).

[64] R. Raussendorf, J. Bermejo-Vega, E. Tyhurst, C. Okay, and M. Zurel, "Phase-space-simulation method for quantum computation with magic states on qubits", Phys. Rev. A **101**, 012350 (2020).

[65] P. Shor, in *Proceedings 35th Annual Symposium on Foundations of Computer Science* (1994) pp. 124–134.

[66] A. Y. Kitaev, "Quantum measurements and the abelian stabilizer problem", arXiv:quant-ph/9511026 [quant-ph] (1995).

[67] M. Ettinger, P. Høyer, and E. Knill, "The quantum query complexity of the hidden subgroup problem is polynomial", Information Processing Letters **91**, 43-48 (2004).

[68] O. Regev, "Quantum computation and lattice problems", SIAM Journal on Computing **33**, 738-760 (2004), https://doi.org/10.1137/S0097539703440678 .

[69] J. M. Farinholt, "An ideal characterization of the clifford operators", J. Phys. A: Math. Theor. **47**, 305303 (2014).

[70] D. Gottesman, "Stabilizer codes and quantum error correction", arXiv:quant-ph/9705052 (1997).

[71] A. Serafini, *Quantum Continuous Variables: A Primer of Theoretical Methods* (CRC press, 2017).

[72] F. M. Dopico and C. R. Johnson, "Parametrization of the Matrix Symplectic Group and Applications", SIAM J. Matrix Anal. Appl. **31**, 650–673 (2009).

[73] C. Zachos, D. Fairlie, and T. Curtright, *Quantum mechanics in phase space: an overview with selected papers* (World Scientific, 2005).

[74] R. Jozsa, "Fidelity for Mixed Quantum States", Journal of Modern Optics **41**, 2315–2323 (1994).

[75] G. De Palma, A. Mari, V. Giovannetti, and A. S. Holevo, "Normal form decomposition for gaussian-to-gaussian superoperators", Journal of Mathematical Physics **56**, 052202 (2015).

[76] C. Weedbrook, S. Pirandola, R. García-Patrón, N. J. Cerf, T. C. Ralph, J. H. Shapiro, and S. Lloyd, "Gaussian quantum information", Rev. Mod. Phys. **84**, 621–669 (2012).

[77] J. Eisert and M. B. Plenio, "Conditions for the local manipulation of gaussian states", Phys. Rev. Lett. **89**, 097901 (2002).

[78] J. Fiurášek, "Gaussian transformations and distillation of entangled gaussian states", Phys. Rev. Lett. **89**, 137904 (2002).

[79] G. Giedke and J. Ignacio Cirac, "Characterization of gaussian operations and distillation of gaussian states", Phys. Rev. A **66**, 032316 (2002).

[80] S. Lloyd and S. L. Braunstein, "Quantum computation over continuous variables", Phys. Rev. Lett. **82**, 1784–1787 (1999).

[81] R. I. Booth, U. Chabaud, and P.-E. Emeriau, "Contextuality and wigner negativity are equivalent for continuous-variable quantum measurements", Phys. Rev. Lett. **129**, 230401 (2022).

[82] A. I. Lvovsky, P. Grangier, A. Ourjoumtsev, V. Parigi, M. Sasaki, and R. Tualle-Brouri, "Production and applications of non-gaussian quantum states of light", arXiv:2006.16985 [quant-ph] (2020).

[83] M. Dakna, J. Clausen, L. Knöll, and D.-G. Welsch, "Erratum: Generation of arbitrary quantum states of traveling fields [phys. rev. a 59, 1658 (1999)]", Phys. Rev. A **60**, 726–726 (1999).

[84] J. Fiurášek, R. García-Patrón, and N. J. Cerf, "Conditional generation of arbitrary single-mode quantum states of light by repeated photon subtractions", Phys. Rev. A **72**, 033822 (2005).

[85] K. Takase, J.-i. Yoshikawa, W. Asavanant, M. Endo, and A. Furusawa, "Generation of optical schrödinger cat states by generalized photon subtraction", Phys. Rev. A **103**, 013710 (2021).

[86] M. Gu, C. Weedbrook, N. C. Menicucci, T. C. Ralph, and P. van Loock, "Quantum computing with continuous-variable clusters", Phys. Rev. A **79**, 062318 (2009).

[87] P. Marek, R. Filip, and A. Furusawa, "Deterministic implementation of weak quantum cubic nonlinearity", Phys. Rev. A **84**, 053802 (2011).

[88] M. Yukawa, K. Miyata, H. Yonezawa, P. Marek, R. Filip, and A. Furusawa, "Emulating quantum cubic nonlinearity", Phys. Rev. A **88**, 053816 (2013).

[89] K. Marshall, R. Pooser, G. Siopsis, and C. Weedbrook, "Repeat-until-success cubic phase gate for universal continuous-variable quantum computation", Phys. Rev. A **91**, 032321 (2015).

[90] K. Miyata, H. Ogawa, P. Marek, R. Filip, H. Yonezawa, J.-i. Yoshikawa, and A. Furusawa, "Implementation of a quantum cubic gate by an adaptive non-gaussian measurement", Phys. Rev. A **93**, 022301 (2016).

[91] P. Marek, R. Filip, H. Ogawa, A. Sakaguchi, S. Takeda, J.-i. Yoshikawa, and A. Furusawa, "General implementation of arbitrary nonlinear quadrature phase gates", Phys. Rev. A **97**, 022329 (2018).

[92] F. Arzani, N. Treps, and G. Ferrini, "Polynomial approximation of non-Gaussian unitaries by counting one photon at a time", Physical Review A **95**, 052352 (2017).

[93] M. Brunelli, O. Houhou, D. W. Moore, A. Nunnenkamp, M. Paternostro, and A. Ferraro, "Unconditional preparation of nonclassical states via linear-and-quadratic optomechanics", Phys. Rev. A **98**, 063801 (2018).

[94] M. Brunelli and O. Houhou, "Linear and quadratic reservoir engineering of non-Gaussian states", Physical Review A **100**, 013831 (2019).

[95] K. K. Sabapathy, H. Qi, J. Izaac, and C. Weedbrook, "Production of photonic universal quantum gates enhanced by machine learning", Physical Review A **100**, 012326 (2019).

[96] R. Yanagimoto, T. Onodera, E. Ng, L. G. Wright, P. L. McMahon, and H. Mabuchi, "Engineering a Kerr-based Deterministic Cubic Phase Gate via Gaussian Operations", Physical Review Letters **124**, 240503 (2019).

[97] O. Houhou, D. W. Moore, S. Bose, and A. Ferraro, "Unconditional measurement-based quantum computation with optomechanical continuous variables", arXiv:1809.09733 (2018).

[98] M. Kudra, M. Kervinen, I. Strandberg, S. Ahmed, M. Scigliuzzo, A. Osman, D. P. Lozano, M. O. Tholén, R. Borgani, D. B. Haviland, G. Ferrini, J. Bylander, A. F. Kockum, F. Quijandría, P. Delsing, and S. Gasparinetti, "Robust preparation of wigner-negative states with optimized snap-displacement sequences", PRX Quantum **3**, 030301 (2022).

[99] C. W. S. Chang, C. Sabín, P. Forn-Díaz, F. Quijandría, A. M. Vadiraj, I. Nsanzineza, G. Johansson, and C. M. Wilson, "Observation of three-photon spontaneous parametric down-conversion in a superconducting parametric cavity", Phys. Rev. X **10**, 011011 (2020).

[100] S. L. Braunstein and R. I. McLachlan, "Generalized squeezing", Physical Review A **35**, 1659–1667 (1987).

[101] K. Banaszek and P. L. Knight, "Quantum interference in three-photon down-conversion", Physical Review A **55**, 2368–2375 (1997).

[102] D. Gottesman, A. Kitaev, and J. Preskill, "Encoding a qubit in an oscillator", Phys. Rev. A **64**, 012310 (2001).

[103] V. V. Albert, K. Noh, K. Duivenvoorden, D. J. Young, R. T. Brierley, P. Reinhold, C. Vuillot, L. Li, C. Shen, S. M. Girvin, B. M. Terhal, and L. Jiang, "Performance and structure of single-mode bosonic codes", Phys. Rev. A **97**, 032346 (2018).

[104] T. Hillmann, F. Quijandría, A. L. Grimsmo, and G. Ferrini, "Performance of teleportation-based error-correction circuits for bosonic codes with noisy measurements", PRX Quantum **3**, 020334 (2022).

[105] L. Hu, Y. Ma, W. Cai, X. Mu, Y. Xu, W. Wang, Y. Wu, H. Wang, Y. Song, C.-L. Zou, *et al.*, "Quantum error correction and universal gate set operation on a binomial bosonic logical qubit", Nature Physics **15**, 503–508 (2019).

[106] S. Rosenblum, P. Reinhold, M. Mirrahimi, L. Jiang, L. Frunzio, and R. J. Schoelkopf, "Fault-tolerant detection of a quantum error", Science **361**, 266-270 (2018), https://www.science.org/doi/pdf/10.1126/science.aat3996 .

[107] S. Rosenblum, Y. Y. Gao, P. Reinhold, C. Wang, C. J. Axline, L. Frunzio, S. M. Girvin, L. Jiang, M. Mirrahimi, M. H. Devoret, *et al.*, "A cnot gate between multiphoton qubits encoded in two cavities", Nature communications **9**, 1–6 (2018).

[108] E. Chitambar and G. Gour, "Quantum resource theories", Rev. Mod. Phys. **91**, 025001 (2019).

[109] N. Gisin, G. Ribordy, W. Tittel, and H. Zbinden, "Quantum cryptography", Rev. Mod. Phys. **74**, 145–195 (2002).

[110] V. Giovannetti, S. Lloyd, and L. Maccone, "Advances in quantum metrology", Nature Photonics **5**, 222–229 (2011).

[111] N. Gisin and R. Thew, "Quantum communication", Nature Photonics **1**, 165–171 (2007).

[112] S. Pirandola, J. Eisert, C. Weedbrook, A. Furusawa, and S. L. Braunstein, "Advances in quantum teleportation", Nature Photonics **9**, 641-652 (2015).

[113] M. Howard, J. Wallman, V. Veitch, and J. Emerson, "Contextuality supplies the 'magic' for quantum computation", Nature **510**, 351-355 (2014).

[114] S. Bravyi and A. Kitaev, "Universal quantum computation with ideal Clifford gates and noisy ancillas", Physical Review A **71**, 022316 (2005).

[115] H. Pashayan, J. J. Wallman, and S. D. Bartlett, "Estimating outcome probabilities of quantum circuits using quasiprobabilities", Phys. Rev. Lett. **115**, 070501 (2015).

[116] K. E. Cahill and R. J. Glauber, "Ordered expansions in boson amplitude operators", Phys. Rev. **177**, 1857–1881 (1969).

[117] S. Glancy and H. M. de Vasconcelos, "Methods for producing optical coherent state superpositions", JOSA B **25**, 712–733 (2008).